

product indicate the composition  $[M(\text{dien})_2]^{2+}[\text{HOC}(\text{CF}_3)_2\text{O}^-]_2$ , in which the metal is complexed by two triamine ligands to give a large, stable dication with octahedral coordination. The structure of the fluorinated anion is unclear; it is different from that reported previously by Roesky et al. where the complex dianion  $[\text{H}_2\{\text{OC}(\text{CF}_3)_2\text{OH}\}^{2-}]$  contains four diol residues.<sup>11</sup> Since the latter had been made by the hydrolysis of the anion  $[(\text{CF}_3)_2\text{C}=\text{NC}(\text{CF}_3)_2\text{O}^-]$ , we repeated the synthesis by the direct reaction of aqueous  $(\text{CF}_3)_2\text{C}(\text{OH})_2$  with base in the presence of large cations ( $\text{Et}_4\text{N}^+$ ,  $\text{Ph}_4\text{P}^+$ ,  $\text{Ph}_4\text{As}^+$ ); in each case, the product isolated contained the same  $[\text{H}_2\{\text{OC}(\text{CF}_3)_2\text{OH}\}_4^{2-}]$  dianion. It seems likely that the structure of the loosely bonded free anion formed from the diol is easily influenced by the nature of the counterion present, and investigation of this point is continuing.

### Conclusions

These results clearly establish the preferred modes of coordination of hexafluoropropane-2,2-diol. In the diionized form, it chelates to a variety of metal ions, with bridging found only with ions such as  $\text{Au}^+$ , where the formation of small rings is disfavored. The reduction of basicity of the alkoxides accompanying fluorination causes them to coordinate to one metal center only; it is

not surprising this ligand does not form a polyoxomolybdate cluster complex analogous to that derived from  $\text{CH}_2(\text{OH})_2$ .<sup>2</sup> The formation of complexes containing six-membered rings results from the increased stability of the ethereal linkage found in fluorinated systems and the ease with which it is formed by a template condensation reaction.

We conclude that the ready availability and unique properties of  $(\text{CF}_3)_2\text{C}(\text{OH})_2$  make it particularly suitable for reaction with a large variety of metal ions to produce stable complexes.

**Acknowledgment.** Financial support of this work was provided by the Natural Sciences and Engineering Research Council of Canada in the form of operating grants to N.C.P. and C.J.W. and a graduate scholarship to R.C.H.

**Supplementary Material Available:** Tables of analytical data, hydrogen atom parameters, anisotropic thermal parameters, additional intramolecular dimensions, selected torsion angles, a weighted least-squares plane, and atomic and thermal parameters (12 pages); listings of calculated and observed structure factors (38 pages). Ordering information is available on any current masthead page.

## Subsite-Differentiated Analogues of Native $[4\text{Fe}-4\text{S}]^{2+}$ Clusters: Preparation of Clusters with Five- and Six-Coordinate Subsites and Modulation of Redox Potentials and Charge Distributions

S. Ciurli,<sup>1a</sup> M. Carrié,<sup>1a</sup> J. A. Weigel,<sup>1a</sup> M. J. Carney,<sup>1a</sup> T. D. P. Stack,<sup>1a</sup> G. C. Papaefthymiou,<sup>1b</sup> and R. H. Holm\*,<sup>1a</sup>

Contribution from the Department of Chemistry, Harvard University, Cambridge, Massachusetts 02138, and the Francis Bitter National Magnet Laboratory, Massachusetts Institute of Technology, Cambridge, Massachusetts 02139. Received September 11, 1989

**Abstract:** The subsite-differentiated cluster  $[\text{Fe}_4\text{S}_4(\text{LS}_3)\text{Cl}]^{2-}$  (**1**,  $\text{LS}_3 = 1,3,5\text{-tris}((4,6\text{-dimethyl-3-mercaptophenyl})\text{thio})\text{-}2,4,6\text{-tris}(p\text{-tolylthio})\text{benzene}(3\text{-})$ ) in  $\text{Me}_2\text{SO}$  solution reacts with a variety of bidentate and tridentate ligands to afford the substituted clusters  $[\text{Fe}_4\text{S}_4(\text{LS}_3)\text{L}]^{z-}$ . Some ten clusters of this type were prepared in order to examine the effects of cluster charge and coordination number at the unique subsite on relative stabilities of oxidation states and charge distributions as sensed by <sup>57</sup>Fe isomer shifts. This is the first comprehensive study of such effects with  $\text{Fe}_4\text{S}_4$  clusters. Clusters prepared include those with  $\text{L}' = \text{PhS}^-$  (**4**),  $\text{Me}_2\text{NCS}_2^-$  (**5**), pyridine-2-thiolate (**6**), 1,4,7-triazacyclononane (**8**), hydrotris(1-pyrazolyl)borate (**9**), and 1,2-disubstituted benzenes such as benzene-1,2-dithiolate (**11**). Cluster formation is detected by <sup>1</sup>H NMR isotropic shifts of the  $\text{LS}_3$  ligand, which are highly sensitive to  $\text{L}'$ . A tabulation of shifts is presented. All clusters have effective trigonal symmetry in solution. Among the more significant properties of the substituted clusters are the following: (i) chemically reversible  $[\text{Fe}_4\text{S}_4]^{3+/2+}$  redox couples at potentials ca. 300–700 mV more negative than that of reference cluster **4**; (ii) negative shifts of the potentials of the  $[\text{Fe}_4\text{S}_4]^{3+/2+}$  and  $[\text{Fe}_4\text{S}_4]^{2+/+}$  couples on mononegative cluster **8** vs **1** and **4**; and (iii) skewing of electron distribution at the unique subsites toward “ferric-like” (**5**, **6**, **11**) and “ferrous-like” (**8**, **9**) character vs symmetrically delocalized **4**. Other matters considered include the source of stability of certain substituted clusters and the effects of cluster charge and core charge density on redox potentials. The data presented approximate the intrinsic effects of various potential ligand sets at a single subsite in native clusters. The possible biological implications of this work are illustrated with the P-clusters of nitrogenase, whose terminal ligation may depart from that of the now-classical native clusters  $\text{Fe}_4\text{S}_4(\text{S-Cys})_4$ .

We have pointed out recently that certain native  $\text{Fe}_4\text{S}_4$  clusters exhibit structural and reactivity features localized at a specific Fe subsite.<sup>2</sup> Examples include the covalently bridged, magnetically coupled cluster-siroheme active site of *E. coli* sulfite reductase,<sup>3,4</sup> the  $\text{Fe}_3\text{S}_4 \rightleftharpoons \text{Fe}_4\text{S}_4$  cluster interconversion in aconitase

where the same subsite is occupied and voided in the two processes,<sup>5–8</sup> and the incorporation of  $\text{Fe}^{2+}$ ,  $\text{Co}^{2+}$ , and  $\text{Zn}^{2+}$  ions in the  $\text{Fe}_3\text{S}_4$  cluster of *Desulfovibrio gigas* ferredoxin II.<sup>9–11</sup> Sub-

(1) (a) Harvard University. (b) M.I.T.

(2) Stack, T. D. P.; Holm, R. H. *J. Am. Chem. Soc.* **1987**, *109*, 2546; **1988**, *110*, 2484.

(3) Christner, J. A.; Janick, P. A.; Siegel, L. M.; Münck, E. *J. Biol. Chem.* **1983**, *258*, 11157.

(4) McRee, D. E.; Richardson, D. C.; Richardson, J. S.; Siegel, L. M. *J. Biol. Chem.* **1986**, *261*, 10277.

(5) Kent, T. A.; Dreyer, J.-L.; Kennedy, M. C.; Huynh, B. H.; Emptage, M. H.; Beinert, H.; Münck, E. *Proc. Natl. Acad. Sci. U.S.A.* **1982**, *79*, 1096.

(6) Kent, T. A.; Emptage, M. H.; Merkle, H.; Kennedy, M. C.; Beinert, H.; Münck, E. *J. Biol. Chem.* **1985**, *260*, 6871.

(7) Robbins, A. H.; Stout, C. D. *Proc. Natl. Acad. Sci. U.S.A.* **1989**, *86*, 3639; *Proteins* **1989**, *5*, 289.

(8) Emptage, M. H. In *Metal Clusters in Proteins*; Que, L., Jr., Ed.; ACS Symp. Ser. 392; American Chemical Society: Washington, DC, 1988; Chapter 17.

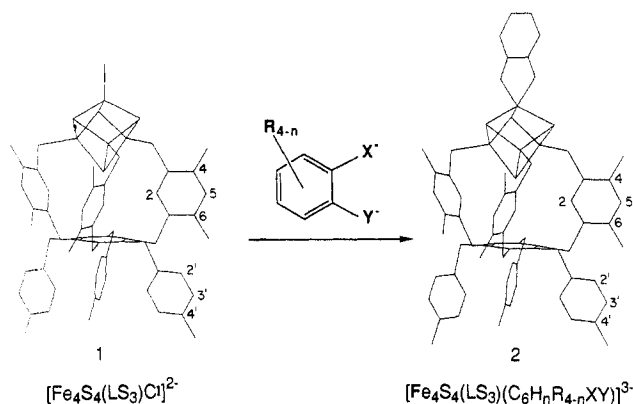


**Figure 1.** Schematic illustration of the subsite-specific binding of bidentate ligands of the type  $(\text{C}_6\text{H}_4\text{XY})^{2-}$  ( $\text{X}, \text{Y} = \text{O}, \text{S}$ ) by chloride displacement from  $[\text{Fe}_4\text{S}_4(\text{LS}_3)\text{Cl}]^{2-}$  (1) to yield the generalized clusters  $[\text{Fe}_4\text{S}_4(\text{LS}_3)(\text{C}_6\text{H}_4\text{R}_{4-n}\text{XY})]^{3-}$  (2,  $\text{R} = \text{H}, \text{Cl}, \text{Me}$ ). The trigonally symmetric conformations of 1 and 2 (excluding the bidentate ligand) were drawn from the coordinates of  $[\text{Fe}_4\text{Se}_4(\text{LS}_3)\text{Cl}]^{2-}$ , which has imposed trigonal symmetry as its  $\text{Ph}_4\text{P}^+$  salt.<sup>13</sup>

site-specific properties of  $\text{Fe}_4\text{S}_4$  clusters in proteins are considered at some length elsewhere.<sup>12</sup>

In order to meet the requirement of subsite differentiation in a cluster appropriate for the examination of reactions and structures at a single subsite by the synthetic analogue approach, the tridentate ligand  $\text{L}(\text{SH})_3$  has been prepared.<sup>2,13,14</sup> The trithiol reacts with  $[\text{Fe}_4\text{S}_4(\text{SEt})_4]^{2-}$  to yield  $[\text{Fe}_4\text{S}_4(\text{LS}_3)(\text{SEt})]^{2-}$ . This compound with 1 equiv of pivaloyl chloride affords  $[\text{Fe}_4\text{S}_4(\text{LS}_3)\text{Cl}]^{2-}$  (1), in which the desired 1:3 subsite differentiation has been demonstrated by an X-ray structure determination.<sup>2</sup> The  $^1\text{H}$  NMR spectrum of this cluster is consistent with a solution structure of effective trigonal symmetry,<sup>2</sup> which is schematically illustrated in Figure 1. Because cluster 1 is susceptible to substitution, it has proven possible to prepare clusters with a wide variety of ligands at the unique subsite. One type of substitution reaction affording clusters of type 2 with five-coordinate subsites is illustrated in Figure 1. Facile ligand substitution leads to a number of applications of site-differentiated clusters. One such application is the formation of bridged double-cubane clusters and the examination of subcluster interactions as manifested by deviations of redox potentials from statistical behavior.<sup>15</sup> In another case, binding of three alkylisonitrile ligands at the unique subsite induces the formation of low-spin Fe(II) and the consequent spin-isolation of a  $[\text{Fe}_3\text{S}_4]^{10}$  cluster fragment whose  $S = 2$  ground state has been spectroscopically characterized.<sup>16</sup> Consequently, appropriate substitution at one subsite can modulate electron distribution and spin-coupling within the  $[\text{Fe}_4\text{S}_4]^{2+}$  core.

The foregoing observations suggest that other stereoelectronic variables can be examined with subsite-differentiated clusters. Among these are coordination number at the unique site and the

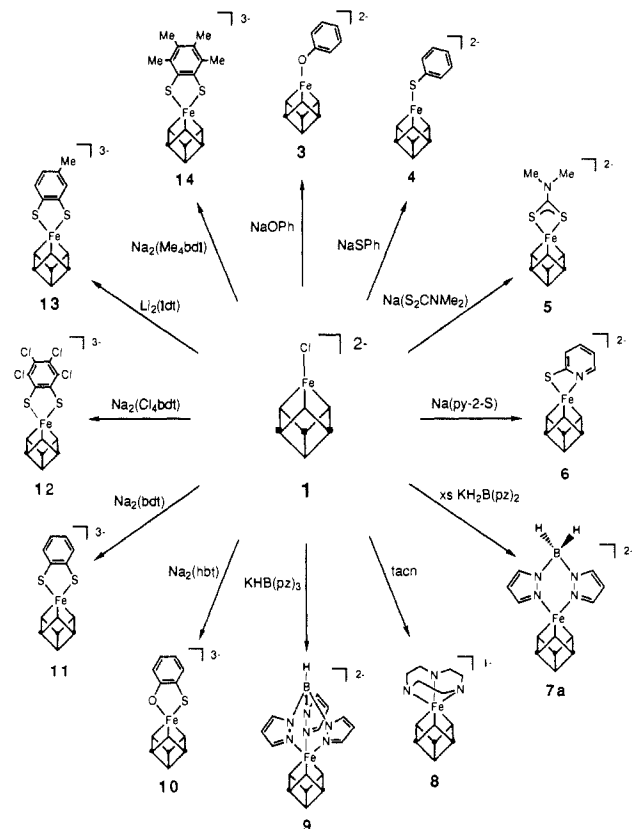


**Figure 2.** Reaction scheme showing the preparations of clusters 3–14 from 1 by chloride displacement. The Fe-containing cube symbolizes the  $\text{Fe}_4\text{S}_4(\text{LS}_3)$  portion of a  $[\text{Fe}_4\text{S}_4(\text{LS}_3)\text{L}']^{n-}$  cluster.

attendant cluster overall charge. Very few  $\text{Fe}_4\text{S}_4$  clusters having one or more subsites exceeding coordination number 4 have been prepared. The  $\text{Et}_4\text{N}^+$  salt of  $[\text{Fe}_4\text{S}_4(\text{SC}_6\text{H}_4\text{-}o\text{-OH})_4]^{2-}$  has one five-coordinate subsite per cluster in the solid state, but in solution all subsites become four-coordinate.<sup>17</sup> The clusters  $[\text{Fe}_4\text{S}_4(\text{S}_2\text{CNEt}_2)_2\text{X}_2]^{2-}$  ( $\text{X} = \text{Cl}^-, \text{PhS}^-$ ) and  $[\text{Fe}_4\text{S}_4(\text{S}_2\text{CNEt}_2)\text{Cl}_3]^{2-}$  have been structurally characterized in the solid state,<sup>18</sup> but they tend to disproportionate in solution. In our earlier work, only unidentate ligands were shown to displace chloride. As demonstrated here, cluster 1 also readily binds bidentate and tridentate ligands at its unique site. Certain of these ligands cause substantial changes in electron distribution as sensed by Mössbauer spectroscopy and, especially, in the relative stabilities of oxidation states. This report describes the preparation and spectroscopic and redox properties of new types of substituted  $[\text{Fe}_4\text{S}_4]^{2+}$  clusters and their possible biological implications.

## Experimental Section

**Preparation of Compounds.**<sup>14</sup> All operations were performed under a pure dinitrogen atmosphere with standard Schlenk techniques or a Vacuum Atmospheres drybox. Acetonitrile was purified by distillation from  $\text{CaH}_2$  and THF from sodium benzophenone. DMF (Burdick & Jackson),  $\text{Me}_2\text{SO}$ , and deuterated solvents were dried over molecular sieves prior to use.  $(\text{Ph}_4\text{P})_2[\text{Fe}_4\text{S}_4(\text{LS}_3)\text{Cl}]^{2-}$  (1),  $(\text{Et}_4\text{N})_2[\text{Fe}_4\text{S}_4\text{Cl}_4]$ ,<sup>19</sup>  $(\text{Et}_4\text{N})_2[\text{Fe}_4\text{S}_4(\text{S}-p\text{-tol})_4]$ ,<sup>20</sup> benzene-1,2-dithiol,<sup>21</sup> tetrachlorobenzene-1,2-dithiol,<sup>22</sup> tetramethylbenzene-1,2-dithiol,<sup>23</sup>  $\text{K}[\text{H}_2\text{B}(\text{pz})_2]$ ,<sup>24</sup>  $\text{K}[\text{HB}(\text{pz})_3]$

(17) Johnson, R. E.; Papaefthymiou, G. C.; Frankel, R. B.; Holm, R. H. *J. Am. Chem. Soc.* **1983**, *105*, 7280.

(18) Kanatzidis, M. G.; Coucouvanis, D.; Simopoulos, A.; Kostikas, A.; Papaefthymiou, V. *J. Am. Chem. Soc.* **1985**, *107*, 4925.

(19) Wong, G. B.; Bobrik, M. A.; Holm, R. H. *Inorg. Chem.* **1978**, *17*, 578.

(20) Averill, B. A.; Herskovitz, T.; Holm, R. H.; Ibers, J. A. *J. Am. Chem. Soc.* **1973**, *95*, 3523.

(21) Testaferri, L.; Tiecco, M.; Tingoli, M.; Chianelli, D.; Montanucci, M. *Synthesis* **1983**, 751.

(22) Baker-Hawkes, M. J.; Billig, E.; Gray, H. B. *J. Am. Chem. Soc.* **1966**, *88*, 4870.

(23) Adams, R.; Ferretti, E. *J. Am. Chem. Soc.* **1959**, *81*, 4927, 4939.

(9) Moura, J. J. G.; Moura, I.; Kent, T. A.; Lipscomb, J. D.; Huynh, B. H.; LeGall, J.; Xavier, A. V.; Münck, E. *J. Biol. Chem.* **1982**, *257*, 6259.

(10) Moura, I.; Moura, J. J. G.; Münck, E.; Papaefthymiou, V.; LeGall, J. *J. Am. Chem. Soc.* **1986**, *108*, 349.

(11) Surerus, K. K.; Münck, E.; Moura, I.; Moura, J. J. G.; LeGall, J. *J. Am. Chem. Soc.* **1987**, *109*, 3805.

(12) Holm, R. H.; Ciurli, S.; Weigel, J. A. *Prog. Inorg. Chem.* To be published.

(13) Stack, T. D. P.; Weigel, J. A.; Holm, R. H. Results to be published.

(14) Abbreviations: bdt, benzene-1,2-dithiolate(2-); Cl<sub>4</sub>bdt, tetrachlorobenzene-1,2-dithiolate(2-); Fc, ferrocene; Fd, ferredoxin; H<sub>2</sub>B(pz)<sub>2</sub>, dihydrobis(1-pyrazolyl)borate(1-); HB(pz)<sub>3</sub>, hydrotris(1-pyrazolyl)borate(1-); hbt, 2-hydroxybenzenethiolate(2-); HP, high-potential protein; L(SH)<sub>3</sub> = 1,3,5-tris((4,6-dimethyl-3-mercaptophenyl)thio)-2,4,6-tris(*p*-tolylthio)benzene; Me<sub>4</sub>bdt, tetramethylbenzene-1,2-dithiolate(2-); Me<sub>3</sub>taen, *N,N',N''*-trimethyl-1,4,7-triazacyclononane; py-2-S, pyridine-2-thiolate(1-); tacn, 1,4,7-triazacyclononane; tdt, toluene-3,4-dithiolate(2-); tol, tolyl.

(15) Stack, T. D. P.; Carney, M. J.; Holm, R. H. *J. Am. Chem. Soc.* **1989**, *111*, 1670.

(16) Weigel, J. A.; Holm, R. H.; Surerus, K. K.; Münck, E. *J. Am. Chem. Soc.* **1989**, *111*, 9246.

(pz)<sub>3</sub>]<sup>24</sup> and K[H<sub>2</sub>B(3,5-Me<sub>2</sub>pz)<sub>2</sub>]<sup>25</sup> were prepared by published methods. All other compounds were commercial samples and were used as received.

A series of cluster compounds **3–14** of the general type [Fe<sub>4</sub>S<sub>4</sub>(LS<sub>3</sub>)-L']<sup>z-</sup>, where *z* = 1, 2, or 3 and L' is a mono-, bi-, or tridentate ligand, were prepared by chloride substitution of cluster **1** in the reactions illustrated in Figure 2. Clusters **3**, **7b**, **11**, and **14** were generated in solution but not isolated. All other clusters were isolated as Ph<sub>4</sub>P<sup>+</sup> salts. In these preparations, volume reduction and drying steps were carried out at ambient temperature under partial vacuum. Sodium salts of thiolate ligands were prepared by the reaction of NaH and the thiol in THF. The lithium salt of toluene-3,4-dithiol was obtained from the dithiol and butyllithium in THF. The cluster compounds were not analyzed because of the small scale of the preparations. Their identity and substantial or full purity were established by <sup>1</sup>H NMR spectra, which were determined in Me<sub>2</sub>SO-*d*<sub>6</sub> at 297 K. An exception is **7a**, which was isolated as a mixture with K[H<sub>2</sub>B(pz)<sub>2</sub>]. Absorption spectra were measured in Me<sub>2</sub>SO solutions. All compounds were isolated as dark brown or black, air-sensitive, microcrystalline solids soluble in DMF and Me<sub>2</sub>SO and, in most cases, somewhat soluble in acetonitrile and dichloromethane.

(Ph<sub>4</sub>P)<sub>2</sub>[Fe<sub>4</sub>S<sub>4</sub>(LS<sub>3</sub>)(OPh)] (**3**). To a solution of 4.40 mg (2.19 μmol) of **1** in 0.5 mL of Me<sub>2</sub>SO-*d*<sub>6</sub> was added 98 μL (1.00 equiv) of a 23 mM solution of (Et<sub>4</sub>N)(OPh) in Me<sub>2</sub>SO-*d*<sub>6</sub>, thereby generating the desired cluster. <sup>1</sup>H NMR (anion): δ 2.22 (4'-Me), 3.72 (4-Me), 3.96 (6-Me), 4.32 (*p*-H), 4.52 (2-H), 6.74 (3'-H), 7.21 (2'-H), 8.24 (5-H), 8.91 (*m*-H).

(Ph<sub>4</sub>P)<sub>2</sub>[Fe<sub>4</sub>S<sub>4</sub>(LS<sub>3</sub>)(SPh)] (**4**). A solution of 13.2 mg (0.100 mmol) of NaSPh in 1 mL of acetonitrile was added to a solution of 200 mg (0.099 mmol) of **1** in 5 mL of acetonitrile. The reaction mixture was stirred for 1 h and filtered, and the filtrate volume was reduced to 2 mL. Addition of 100 mL of ether and storage overnight at -20 °C resulted in the separation of a dark red-brown microcrystalline solid. This material was collected by filtration and washed with ether to afford 105 mg (50%) of product. <sup>1</sup>H NMR (anion): δ 2.19 (4'-Me), 3.65 (4-Me), 3.85 (6-Me), 4.90 (2-H), 5.21 (*p*-H), 5.76 (*o*-H), 6.72 (3'-H), 7.10 (2'-H), 8.13 (5-H + *m*-H). Absorption spectrum: λ<sub>max</sub> (ε<sub>M</sub>) 300 (49 000), 460 (15 000) nm.

(Ph<sub>4</sub>P)<sub>2</sub>[Fe<sub>4</sub>S<sub>4</sub>(LS<sub>3</sub>)(S<sub>2</sub>CNMe<sub>2</sub>)] (**5**). A solution of 26 mg (0.18 mmol) of Na(S<sub>2</sub>CNMe<sub>2</sub>) in 2 mL of acetonitrile was added to a solution of 320 mg (0.16 mmol) of **1** in 20 mL of acetonitrile. The mixture was stirred for 1 h and the solvent was removed. The solid residue was extracted with 3 × 15 mL of acetonitrile, and the volume of the combined extracts was reduced to 25 mL in vacuo. Diffusion of ether into this solution at -20 °C caused separation of a dark brown crystalline material, which was collected by filtration, washed with ether, and dried to give 210 mg (68%) of product. <sup>1</sup>H NMR (anion): δ 2.24 (4'-Me), 3.56 (4-Me), 3.92 (6-Me), 4.65 (2-H), 6.64 (3'-H), 7.19 (2'-H), 7.51 (*N*-Me), 8.25 (5-H). Absorption spectrum: λ<sub>max</sub> (ε<sub>M</sub>) 300 (sh, 54 000), 440 (sh, 12 000) nm.

(Ph<sub>4</sub>P)<sub>2</sub>[Fe<sub>4</sub>S<sub>4</sub>(LS<sub>3</sub>)(py-2-S)] (**6**). A solution of 10.4 mg (0.080 mmol) of sodium pyridine-2-thiolate in 1 mL of acetonitrile was added to a solution of 134 mg (0.067 mmol) of **1** in 2 mL of acetonitrile under continuous stirring. After 10 min the solution was evaporated to dryness and the residue was extracted with 3 × 7 mL of acetonitrile. The combined extracts were reduced to 5 mL. Addition of 20 mL of ether and storage at -20 °C yielded 70 mg (48%) of dark brown microcrystalline product. <sup>1</sup>H NMR (anion): δ 2.23 (4'-Me), 3.64 (4-Me), 3.93 (6-Me), 4.77 (2-H), 6.50 (py-H<sub>bc</sub>), 6.67 (3'-H), 7.16 (2-H), 8.24 (5-H), 10.09 (py-H<sub>ac</sub>), 10.85 (py-H<sub>a</sub>), 12.30 (py-H<sub>d</sub>). Absorption spectrum: λ<sub>max</sub> (ε<sub>M</sub>) 290 (sh, 48 000), 440 (11 000) nm.

(Ph<sub>4</sub>P)<sub>2</sub>[Fe<sub>4</sub>S<sub>4</sub>(LS<sub>3</sub>)(H<sub>2</sub>B(pz)<sub>2</sub>)] (**7a**). To a solution of 100 mg (0.050 mmol) of **1** in 10 mL of acetonitrile was added 40 mg (0.20 mmol) of K[H<sub>2</sub>B(pz)<sub>2</sub>]. After the brown solution was stirred for 10 min, solvent was removed to give a brown powder. The material contained the desired cluster and excess ligand, which was added because the cluster is formed in an equilibrium reaction. It was used for Mössbauer spectroscopy. Because of the lability of the cluster, no attempt was made to obtain a pure solid. <sup>1</sup>H NMR (anion): δ 2.23 (4'-Me), 3.85 (4-Me), 4.11 (6-Me), 6.62 (3'-H), 7.13 (2'-H), 8.41 (5-H), 9.65 (pz-H), 10.35 (pz-H).

(Ph<sub>4</sub>P)<sub>2</sub>[Fe<sub>4</sub>S<sub>4</sub>(LS<sub>3</sub>)(H<sub>2</sub>B(Me<sub>2</sub>pz)<sub>2</sub>)] (**7b**). This cluster was generated in Me<sub>2</sub>SO-*d*<sub>6</sub> solution by the method for **7a** but with use of K[H<sub>2</sub>B(3,5-Me<sub>2</sub>pz)<sub>2</sub>]. <sup>1</sup>H NMR (anion): δ 2.23 (4'-Me), 3.85 (4-Me), 4.15 (6-Me), 4.17 (pz-5Me), 4.53 (2-H), 6.54 (3'-H), 7.07 (2'-H), 8.45 (5-H), 10.89 (pz-4H).

(Ph<sub>4</sub>P)<sub>2</sub>[Fe<sub>4</sub>S<sub>4</sub>(LS<sub>3</sub>)(tacn)] (**8**). To a solution of 125 mg (0.062 mmol) of **1** in 10:1 acetonitrile/DMF (v/v) was added 8.83 mg (0.068 mmol) of tacn. No color change was observed. After the solution was stirred for 5 min, a brown solid began to precipitate. The reaction mixture was

maintained at -20 °C overnight, and the dark solid was collected by filtration, washed with ether, and dried to afford 80 mg (73%) of product as a dark red-brown solid. <sup>1</sup>H NMR (anion): δ 2.24 (4'-Me), 3.87 (4-Me), 4.29 (6-Me), 6.55 (3'-H), 7.13 (2'-H), 8.53 (5-H), 8.67 (CH<sub>2</sub>), 12.89 (CH<sub>2</sub>). Absorption spectrum: λ<sub>max</sub> (ε<sub>M</sub>) 303 (sh, 57 000), 488 (10 400) nm.

(Ph<sub>4</sub>P)<sub>2</sub>[Fe<sub>4</sub>S<sub>4</sub>(LS<sub>3</sub>)(HB(pz)<sub>3</sub>)] (**9**). KHB(pz)<sub>3</sub> (13.8 mg, 0.055 mmol) was added to a solution of 100 mg (0.050 mmol) of **1** in 10:1 acetonitrile/DMF (v/v). No color change was observed. The reaction mixture was stirred for 30 min and filtered, and the filtrate was stored overnight at -20 °C. The dark red-brown microcrystalline material was collected, washed with ether, and dried to give 76 mg (69%) of product. <sup>1</sup>H NMR (anion): δ 2.23 (4'-Me), 3.97 (4-Me), 4.41 (6-Me), 6.48 (3'-H), 7.07 (2'-H), 8.66 (5-H), 10.93 (pz-H), 11.76 (pz-H). Absorption spectrum: λ<sub>max</sub> (ε<sub>M</sub>) 302 (sh, 52 600), 480 (11 500) nm.

(Ph<sub>4</sub>P)<sub>3</sub>[Fe<sub>4</sub>S<sub>4</sub>(LS<sub>3</sub>)(hbt)] (**10**). The disodium salt of *o*-hydroxybenzenethiol (35 mg, 0.21 mmol) was added to a solution of 300 mg (0.15 mmol) of **1** in 10 mL of DMF, and 60 mg (0.16 mmol) of Ph<sub>4</sub>P<sub>3</sub>Cl was added. The mixture was stirred for 15 min and filtered, and 50 mL of ether was added to the filtrate. The mixture was maintained at -20 °C for 2 h. The dark brown microcrystalline solid was collected by filtration, washed with ether, and dried to yield 185 mg (51%) of product. <sup>1</sup>H NMR (anion): δ 2.24 (4'-Me), 3.66 (4-Me), 4.10 (6-Me), 5.43 (hbt-H<sub>b</sub>), 5.83 (hbt-H<sub>a</sub>), 6.65 (3'-H), 7.11 (2'-H), 8.37 (5-H), 9.52 (hbt-H<sub>c</sub>), 10.32 (hbt-H<sub>a</sub>). Absorption spectrum: λ<sub>max</sub> (ε<sub>M</sub>) 300 (60 000), 420 (sh, 13 000) nm.

(Ph<sub>4</sub>P)<sub>3</sub>[Fe<sub>4</sub>S<sub>4</sub>(LS<sub>3</sub>)(bdt)] (**11**). To a solution of 18.3 mg (9.10 μmol) of **1** in 0.5 mL of Me<sub>2</sub>SO-*d*<sub>6</sub> was added 50 μL (1.04 equiv) of a 190 mM solution of Na<sub>2</sub>bdt in Me<sub>2</sub>SO-*d*<sub>6</sub>, thereby generating the desired cluster. <sup>1</sup>H NMR (anion): δ 2.25 (4'-Me), 3.46 (4-Me), 4.06 (6-Me), 6.61 (2'-H), 7.14 (bdt-H<sub>b</sub>), 7.18 (3'-H), 8.32 (5-H), 9.97 (bdt-H<sub>a</sub>).

(Ph<sub>4</sub>P)<sub>3</sub>[Fe<sub>4</sub>S<sub>4</sub>(LS<sub>3</sub>)(Cl<sub>4</sub>bdt)] (**12**). The disodium salt of tetrachlorobenzene-1,2-dithiolate (66 mg, 0.20 mmol) was added to a solution of 300 mg (0.15 mmol) of **1** in 10 mL of DMF, and 67 mg (0.18 mmol) of Ph<sub>4</sub>P<sub>3</sub>Cl was added. After the mixture was stirred for 15 min, 60 mL of ether was added and the mixture was maintained at -20 °C for 2 h; 230 mg of a microcrystalline solid was obtained. Recrystallization of this material by ether diffusion into a filtered DMF solution gave 175 mg (45%) of product as a black microcrystalline solid. <sup>1</sup>H NMR (anion): δ 2.26 (4'-Me), 3.48 (4-Me), 4.01 (6-Me), 4.30 (2-H), 6.63 (3'-H), 7.22 (2'-H), 8.30 (5-H). Absorption spectrum: λ<sub>max</sub> (ε<sub>M</sub>) 295 (sh, 59 000), 430 (sh, 13 000) nm.

(Ph<sub>4</sub>P)<sub>3</sub>[Fe<sub>4</sub>S<sub>4</sub>(LS<sub>3</sub>)(tdt)] (**13**). To a solution containing 195 mg (0.097 mmol) of **1** in 10 mL of acetonitrile were added 0.49 mL of a 0.20 M Ph<sub>4</sub>P<sub>3</sub>Cl solution and 0.30 mL (0.102 mmol) of a 0.34 M Li<sub>2</sub>tdt solution, both in acetonitrile. The reaction mixture was filtered and reduced in volume to ca. 5 mL. Ether (100 mL) was layered on top of the solution. After storage at -20 °C for 2 h, the product was collected by filtration and washed with ether, affording 0.153 g (64%) of a dark brown solid. <sup>1</sup>H NMR (anion): δ 3.42 (tdt-Me), 3.47 (4-Me), 4.08 (6-Me), 4.20 (2-H), 6.62 (2'-H), 6.78 (tdt-H<sub>b</sub>), 7.19 (2'-H), 8.33 (5-H), 9.81 (tdt-H<sub>a</sub>), 10.17 (tdt-H<sub>a</sub>). Absorption spectrum: λ<sub>max</sub> (ε<sub>M</sub>) 303 (53 400), 468 (16 300).

(Ph<sub>4</sub>P)<sub>3</sub>[Fe<sub>4</sub>S<sub>4</sub>(LS<sub>3</sub>)(Me<sub>4</sub>bdt)] (**14**). To a solution of 16.7 mg (8.31 μmol) of **1** in 0.5 mL of Me<sub>2</sub>SO-*d*<sub>6</sub> was added 70 μL (1.08 equiv) of a 128 mM solution of Na<sub>2</sub>(Me<sub>4</sub>bdt) in Me<sub>2</sub>SO-*d*<sub>6</sub>, thereby generating the desired cluster in situ.

**Physical Measurements.** All measurements were performed under strictly anaerobic conditions. Absorption spectra were determined on a Cary 219 spectrophotometer. <sup>1</sup>H NMR spectra were measured on a Brücker AM-500 spectrometer. Electrochemical measurements were recorded in Me<sub>2</sub>SO and dichloromethane solutions with standard PAR instrumentation, a Pt working electrode, a SCE reference electrode, and 0.1 M LiClO<sub>4</sub> (Me<sub>2</sub>SO) or 0.1 M Bu<sub>4</sub>N(PF<sub>6</sub>) (CH<sub>2</sub>Cl<sub>2</sub>) supporting electrolyte. Under these conditions, E<sub>1/2</sub>(Fc<sup>+</sup>/Fc) = +0.460 V (Me<sub>2</sub>SO) and +0.470 V (CH<sub>2</sub>Cl<sub>2</sub>). Coulometric experiments were conducted with use of a Pt mesh electrode. Mössbauer spectra were determined with a constant-acceleration spectrometer equipped with a <sup>57</sup>Co source in a Rh matrix. Zero-field measurements were made at 4.2 K with the spectrometer in the time mode and the source maintained at room temperature. Polycrystalline solids were dispersed in boron nitride powder and sealed in plastic sample holders with epoxy resin. Isomer shifts are reported relative to Fe metal at 4.2 K.

Isotropically shifted <sup>1</sup>H NMR spectra allow cluster identification and assessment of purity. The following chemical shifts (δ) of salts of the ligands in Me<sub>2</sub>SO-*d*<sub>6</sub> were taken as the diamagnetic references for the isotropic shifts in Table I. Certain spectra of ligands and clusters were assigned with use of spin decoupling and 2-D methods. (Et<sub>4</sub>N)(OPh), 5.88 (t, *p*-H), 6.10 (d, *o*-H), 6.71 (t, *m*-H); NaSPh, 6.43 (t, *p*-H), 6.68 (t, *m*-H), 7.03 (d, *o*-H); Na(S<sub>2</sub>CNMe<sub>2</sub>), 3.40; Na(S-2-py), 6.37 (t, H<sub>b</sub>),

(24) Trofimenko, S. *Inorg. Synth.* 1970, 12, 99.(25) Trofimenko, S. *J. Am. Chem. Soc.* 1967, 89, 6288.

Table I. <sup>1</sup>H Isotropic Shifts of [Fe<sub>4</sub>S<sub>4</sub>(LS<sub>3</sub>)L']<sup>2-</sup> Clusters in Me<sub>2</sub>SO-d<sub>6</sub> at 297 K

|    | L'  | shifts, <sup>a</sup> ppm |       |       |  |
|----|---|--------------------------|-------|-------|--|
|    |   | 4-Me                     | 5-H   | 6-Me  | L' <sup>b</sup>  |
| 1  | Cl <sup>-</sup>   | -1.98                    | -1.43 | -1.86 |  |
| 3  | PhO <sup>-</sup>  | -1.90                    | -1.45 | -1.91 | -2.20 ( <i>m</i> -H); +1.56 ( <i>p</i> -H) <sup>c</sup>  |
| 4  | PhS <sup>-</sup>  | -1.83                    | -1.34 | -1.80 | +1.27 ( <i>o</i> -H); -1.45 ( <i>m</i> -H); +1.22 ( <i>p</i> -H)                                   |
| 5  | Me <sub>2</sub> NCS <sub>2</sub> <sup>-</sup>                     | -1.74                    | -1.46 | -1.87 | -4.11 (Me)   |
| 6  | py-2-S <sup>-</sup>   | -1.82                    | -1.45 | -1.88 | <i>d, e</i>  |
| 7a | [H <sub>2</sub> B(pz) <sub>2</sub> ] <sup>-</sup>                 | -2.03                    | -1.62 | -2.06 | <i>d, f</i>  |
| 7b | [H <sub>2</sub> B(Me <sub>2</sub> pz) <sub>2</sub> ] <sup>-</sup> | -2.03                    | -1.66 | -2.10 | -5.47 (4-H); -2.19 (5-Me) <sup>g</sup>   |
| 8  | tacn  | -2.05                    | -1.74 | -2.24 | -6.07; -10.29  |
| 9  | [HB(pz) <sub>3</sub> ] <sup>-</sup>                               | -2.15                    | -1.87 | -2.36 | <i>d, h</i>  |
| 10 | hbt <sup>2-</sup>   | -1.84                    | -1.58 | -2.05 | -3.35 (H <sub>a</sub> ); +0.39 (H <sub>b</sub> ); -3.27 (H <sub>c</sub> ); +0.27 (H <sub>d</sub> ) |
| 11 | bdt <sup>2-</sup>   | -1.65                    | -1.54 | -2.02 | -2.89 (H <sub>a</sub> ); -1.05 (H <sub>b</sub> )   |
| 12 | Cl <sub>4</sub> bdt <sup>2-</sup>                                 | -1.65                    | -1.50 | -1.96 |  |
| 13 | tdt <sup>2-</sup>   | -1.65                    | -1.54 | -2.03 | -1.49 (Me); -0.86 (H <sub>b</sub> )<br>-2.86 (H <sub>c</sub> ); -3.24 (H <sub>a</sub> )            |
| 14 | Me <sub>4</sub> bdt <sup>2-</sup>                                 | -2.19                    | -2.02 | -2.56 | -1.81 (Me <sub>b</sub> ); -2.23 (Me <sub>a</sub> )   |

<sup>a</sup>(ΔH/H<sub>0</sub>)<sub>iso</sub> = (ΔH/H<sub>0</sub>)<sub>dia</sub> - (ΔH/H<sub>0</sub>)<sub>obs</sub>. <sup>b</sup>Ligand positions illustrated in Figures 5-9. <sup>c</sup>*o*-H signal not located. <sup>d</sup>Definite assignments not made. <sup>e</sup>See Figure 6 for chemical shifts. <sup>f</sup>Chemical shifts, 9.65, 10.35 ppm; 3-H signal assignment uncertain. <sup>g</sup>3-Me signal assignment uncertain. <sup>h</sup>See Figure 7 for chemical shifts.

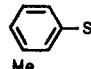
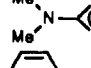
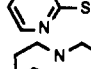
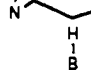
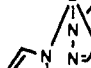
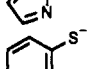
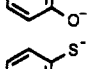
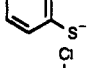
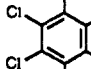
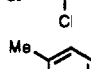
6.89 (t, H<sub>c</sub>), 6.98 (d, H<sub>d</sub>), 7.79 (d, H<sub>a</sub>); K[H<sub>2</sub>B(pz)<sub>2</sub>], 5.90 (d, 4-H), 7.18 + 7.29 (d, d, 3-, 5-H); K[H<sub>2</sub>B(Me<sub>2</sub>pz)<sub>2</sub>], 1.98 + 2.14 (3-, 5-Me), 5.42 (4-H); tacn, 2.60; K[HB(pz)<sub>3</sub>], 5.98 (d, 4-H), 7.28 + 7.31 (d, d, 3-, 5-H); Na<sub>2</sub>(hbt), 5.82 (t, H<sub>b</sub>), 6.10 (d, H<sub>d</sub>), 6.25 (t, H<sub>c</sub>), 6.97 (d, H<sub>a</sub>); Na<sub>2</sub>(bdt), 6.09 (m, H<sub>b</sub>), 7.08 (m, H<sub>a</sub>); Na<sub>2</sub>(tdt), 1.93 (s, Me), 5.92 (d, H<sub>b</sub>), 6.93 (s, H<sub>a</sub>), 6.95 (d, H<sub>c</sub>); Na<sub>2</sub>(Me<sub>4</sub>bdt), 2.01 (Me<sub>b</sub>), 2.44 (Me<sub>a</sub>); Na<sub>3</sub>(LS<sub>3</sub>), 1.82 (4-Me), 2.05 (6-Me), 2.24 (4'-Me), 6.49 (2-H), 6.79 (5-H), 6.80 (d, 3'-H), 7.05 (d, 2'-H).

## Results and Discussion

**Preparation of Clusters.** Previously, we have shown that cluster **1** undergoes stoichiometric substitution reactions with thiolates to afford the products [Fe<sub>4</sub>S<sub>4</sub>(LS<sub>3</sub>)(SR)]<sup>2-</sup>.<sup>2,15</sup> Here it is demonstrated that the unique subsite in cluster **1** is susceptible to substitution by a wide variety of ligands, including bidentates and tridentates. The reactions leading to clusters **3-14** are set out in Figure 2. Clusters of type **2** (**10-14**) are prepared by the reaction in Figure 1, which also introduces the ligand numbering scheme for <sup>1</sup>H NMR spectra. Clusters **3, 7b, 11,** and **14** were generated from **1** in Me<sub>2</sub>SO solutions. As shown in Table II, the potential of the [Fe<sub>4</sub>S<sub>4</sub>]<sup>2+/+</sup> couple of **1** in Me<sub>2</sub>SO is substantially less negative than that in DMF. Further, the cyclic voltammograms are broad (ΔE<sub>p</sub> ≈ 150-220 mV at 50 mV/s). In the presence of a 200-fold excess of chloride, the wave sharpens (ΔE<sub>p</sub> = 100 mV) and shifts to -0.90 V. Consequently, the reactive species in Me<sub>2</sub>SO may be both the chloride-bound and solvated forms in equilibrium. All other clusters were prepared in acetonitrile or DMF, where chloride remains bound. Clusters **7a** and **7b** are formed in equilibrium reactions requiring ca. 4-fold excess of ligand for completion. All other species (except **14**) are produced in reactions with near-stoichiometric amounts of ligand, which are immediate and, when monitored by <sup>1</sup>H NMR, were found to proceed essentially quantitatively in situ.

Clusters **3** and **4** carry unidentate ligands at the unique site and are useful for comparison purposes with themselves and other species. Clusters **5-7** and **10-14** possess five-coordinate subsites and are among the very few [Fe<sub>4</sub>S<sub>4</sub>]<sup>2+</sup> species with this property.<sup>17,18</sup> Clusters **8** and **9**, together with [Fe<sub>4</sub>S<sub>4</sub>(LS<sub>3</sub>)(RNC)<sub>3</sub>]<sup>-</sup>,<sup>16</sup> are the only examples with six-coordinate subsites. Formations of **3-9** proceed cleanly with no NMR-detectable byproducts. With **10, 12,** and **13**, isolation was occasionally accompanied by the formation of small amounts (<5% of total cluster) of the previously reported μ-sulfido double cubane {[Fe<sub>4</sub>S<sub>4</sub>(LS<sub>3</sub>)<sub>2</sub>S]<sup>4-</sup>.<sup>15</sup> This species is readily recognized by its 5-H shift at 8.61 ppm.<sup>15</sup> Generation in situ of **10-13** affords solutions free of this impurity. In view of the accessibility of **12** and **13**, dithiolate cluster **11** was generated in solution but not isolated. Attempted isolation of **7a** led to appreciable conversion to the μ-sulfido species. Generation of cluster **14** was accompanied by formation of an appreciable amount of a paramagnetic byproduct, identified by <sup>1</sup>H NMR as [Fe(Me<sub>4</sub>bdt)<sub>2</sub>(Me<sub>2</sub>SO)<sub>n</sub>]<sup>-</sup>. This complex, with methyl signals at 1.87 and 22.7 ppm, is analogous to known [Fe(bdt)<sub>2</sub>(Me<sub>2</sub>SO)<sub>n</sub>]<sup>-</sup>,<sup>26</sup>

Table II. Redox Potentials of [Fe<sub>4</sub>S<sub>4</sub>(LS<sub>3</sub>)L']<sup>2-</sup> Clusters

| cluster | L'   | solvent                         | E <sub>1/2</sub> , <sup>a</sup> V                  |   |
|---------|--|---------------------------------|--|---|
|         |  |                                 | [Fe <sub>4</sub> S <sub>4</sub> ] <sup>3+/2+</sup> | [Fe <sub>4</sub> S <sub>4</sub> ] <sup>2+/+</sup> |
| 1       | Cl <sup>-</sup>  | Me <sub>2</sub> SO              | <i>b</i>   | -0.90 <sup>c,d</sup>                              |
|         |  | CH <sub>2</sub> Cl <sub>2</sub> | +0.22  | -1.03   |
| 4       |    | Me <sub>2</sub> SO              | <i>b</i>   | -0.97   |
|         |  | CH <sub>2</sub> Cl <sub>2</sub> | +0.02  | -1.15   |
| 5       |   | Me <sub>2</sub> SO              | -0.09  | <i>b</i>  |
|         |  | CH <sub>2</sub> Cl <sub>2</sub> | -0.23  | -1.27   |
| 6       |  | Me <sub>2</sub> SO              | <i>b</i>   | -0.99   |
|         |  | CH <sub>2</sub> Cl <sub>2</sub> | -0.08  | -1.15   |
| 8       |  | Me <sub>2</sub> SO              | -0.01  | -1.13   |
|         |  | CH <sub>2</sub> Cl <sub>2</sub> | -0.09  | -1.22   |
| 9       |  | Me <sub>2</sub> SO              | <i>b</i>   | <i>b</i>  |
|         |  | CH <sub>2</sub> Cl <sub>2</sub> | -0.23  | -1.40   |
| 10      |  | Me <sub>2</sub> SO              | -0.43  | -1.26   |
|         |  |                                 |  |   |
| 11      |  | Me <sub>2</sub> SO              | -0.62  | -1.38   |
|         |  |                                 |  |   |
| 12      |  | Me <sub>2</sub> SO              | -0.48  | -1.27   |
|         |  |                                 |  |   |
| 13      |  | Me <sub>2</sub> SO              | -0.66  | -1.38   |
|         |  |                                 |  |   |
| 14      |  | Me <sub>2</sub> SO              | -0.75  | -1.42   |
|         |  |                                 |  |   |

<sup>a</sup>E<sub>p</sub> = (E<sub>p,c</sub> + E<sub>p,a</sub>)/2 vs SCE at 297 K. <sup>b</sup>Poorly defined, irreversible step. <sup>c</sup>0.1 M Et<sub>4</sub>NCl. <sup>d</sup>E<sub>1/2</sub> = -0.83 (0.1 M Bu<sub>4</sub>NClO<sub>4</sub>), -0.86 (0.1 M LiClO<sub>4</sub>), -1.02 V (DMF, 0.1 M Bu<sub>4</sub>NClO<sub>4</sub>). All potentials refer to ca. 0.5 mM solutions.

and it may be independently generated in solution by the reaction of FeCl<sub>3</sub> and 2 equiv of Na<sub>2</sub>(Me<sub>4</sub>bdt). Because we were unable to eliminate formation of byproducts, no attempts to isolate **7a**

(26) Kang, B. S.; Weng, L. H.; Wu, D. X.; Wang, F.; Guo, Z.; Huang, L. R.; Huang, Z. Y.; Liu, H. Q. *Inorg. Chem.* **1988**, *27*, 1130. In this reference, solutions in Me<sub>2</sub>SO prepared from authentic (Et<sub>4</sub>N)<sub>2</sub>[Fe<sub>2</sub>(bdt)<sub>4</sub>] have been shown to contain the mononuclear species [Fe(bdt)<sub>2</sub>(Me<sub>2</sub>SO)<sub>n</sub>]<sup>-</sup> (*n* = 1 or 2) with an apparent spin *S* = 3/2.

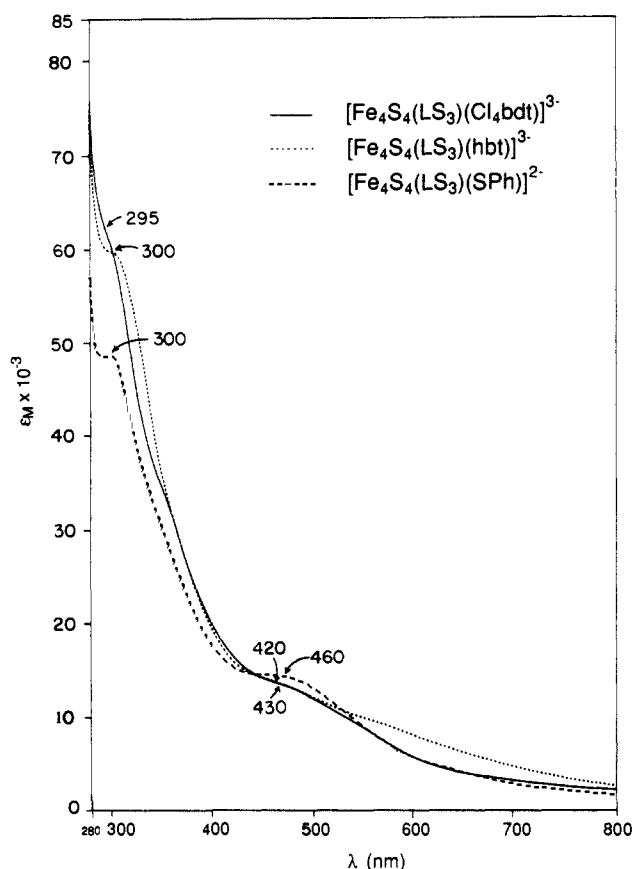


Figure 3. UV-vis absorption spectra of clusters 4, 10, and 12 in Me<sub>2</sub>SO solutions.

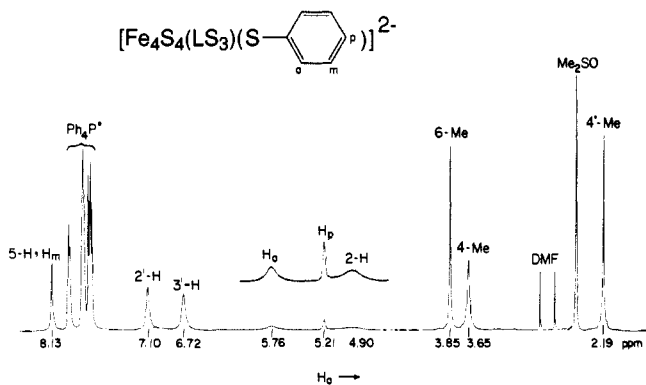


Figure 4. <sup>1</sup>H NMR spectrum of cluster 4 in Me<sub>2</sub>SO-*d*<sub>6</sub> solution at 297 K. Signal assignments are indicated.

or 14 as pure compounds were made.<sup>27</sup>

Certain potential ligands did not react or react cleanly with cluster 1 in Me<sub>2</sub>SO solution. Excess 1,4,7-trithiacyclononane<sup>28</sup> did not displace chloride although it is known to form stable Fe(II,III) complexes, in one instance by reaction with FeCl<sub>2</sub> in methanol.<sup>29</sup> Cluster 1 also did not react with excess bis(2-imidazolyl)nitromethane.<sup>30</sup> With sodium salts of the alkyldithiols *trans*-cyclohexane-1,2-dithiol<sup>31</sup> and bicyclo[2.2.1]hepta-*exo-cis*-2,3-dithiol,<sup>32</sup> complicated mixtures of unidentified products were obtained.

**Identification of Clusters.** A number of the clusters in Figure 2 were isolated as Ph<sub>4</sub>P<sup>+</sup> salts; none yielded diffraction-quality

(27) Clusters 10–13 must be used within a week after isolation as a solid or within 1 day after generation in solution inasmuch as they tend to decompose.

(28) Blower, P. J.; Cooper, S. R. *Inorg. Chem.* **1987**, *26*, 2009.

(29) Wiegardt, K.; Küppers, H.-J.; Weiss, J. *Inorg. Chem.* **1985**, *24*, 3067.

(30) Joseph, M.; Leigh, T.; Swain, M. L. *Synthesis* **1977**, 459.

(31) Willett, J. D.; Grunwell, J. R.; Berchtold, G. A. *J. Org. Chem.* **1968**, *33*, 2297.

(32) Bartlett, P. D.; Ghosh, T. *J. Org. Chem.* **1987**, *52*, 4937.

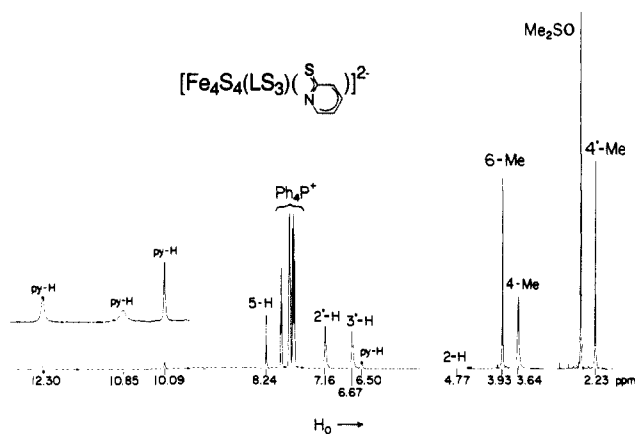


Figure 5. <sup>1</sup>H NMR spectrum of cluster 6 in Me<sub>2</sub>SO-*d*<sub>6</sub> solution at 297 K. Signal assignments are indicated.

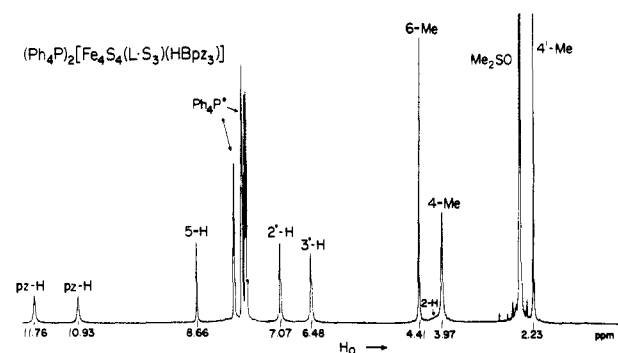


Figure 6. <sup>1</sup>H NMR spectrum of cluster 9 in Me<sub>2</sub>SO-*d*<sub>6</sub> solution at 297 K. Signal assignments are indicated.

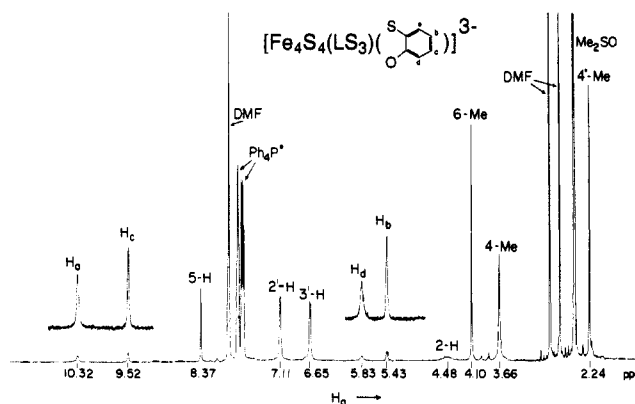


Figure 7. <sup>1</sup>H NMR spectrum of cluster 10 in Me<sub>2</sub>SO-*d*<sub>6</sub> solution at 297 K. Signal assignments are indicated.

crystals. Cluster identification follows from spectroscopic properties. As illustrated in Figure 3 for 4, 10, and 12, product clusters lack the prominent absorption band of precursor 1 at 490 nm.<sup>2,33</sup> Further, the spectra of 10 and 12 are blue-shifted compared to 4, suggesting a different ligation mode at the unique subsite. Unambiguous identification of the clusters can be made from their isotropically shifted <sup>1</sup>H NMR spectra, in which the isotropic shifts of substituents at the 4-, 5-, and 6-positions of the ligand (Figure 1) are extremely sensitive to the identity of the ligand at the unique subsite. Clusters containing the [Fe<sub>4</sub>S<sub>4</sub>]<sup>2+</sup> core exhibit contact shifts resulting from ligand-to-metal antiparallel spin transfer.<sup>34</sup>

(33) The only exception is 8, for which λ<sub>max</sub> = 488 nm. This cluster has been identified by its <sup>1</sup>H NMR spectrum (vide infra).

(34) (a) Holm, R. H.; Phillips, W. D.; Averill, B. A.; Mayerle, J. J.; Herskovitz, T. *J. Am. Chem. Soc.* **1974**, *96*, 2109. (b) Reynolds, J. G.; Laskowski, E. J.; Holm, R. H. *J. Am. Chem. Soc.* **1978**, *100*, 5315. Isotropic shifts arise from thermal occupation of excited states of the spin ladder with *S* > 0.

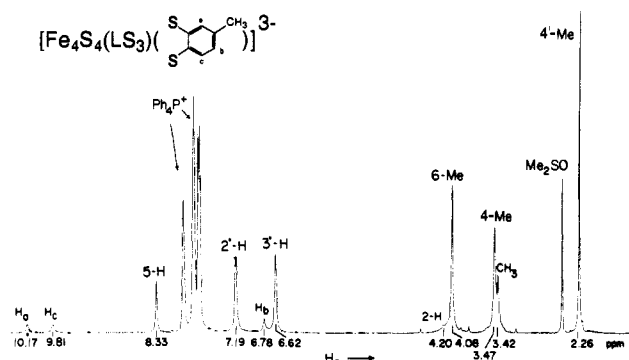


Figure 8. <sup>1</sup>H NMR spectrum of cluster **13** in Me<sub>2</sub>SO-*d*<sub>6</sub> solution at 297 K. Signal assignments are indicated.

Isotropic shifts, calculated from ligand anion chemical shifts, are collected in Table I.<sup>35</sup> They are indicative of an *S* = 0 ground state for all clusters. Shifts at the foregoing positions are precise to ±0.01 ppm owing to the narrow line widths. Structural identification is exemplified by the NMR spectra in Figures 4–8. The spectrum of **4** in Figure 4 provides a useful reference. It and the spectra of all other clusters examined in this work and previously<sup>2,15,16</sup> are consistent with a trigonally symmetric LS<sub>3</sub> ligand conformation, as illustrated for **1** and **2** in Figure 1.

Dominant contact shifts are clearly demonstrated by the alternating signs of the isotropic shifts around the rings of PhO<sup>-</sup> (**3**) and PhS<sup>-</sup> (**4**) ligands, and the same sign of shifts of 4-Me, 5-H, and 6-Me on the coordinating arms of the ligand. These rings are odd-alternate systems in spin delocalization. Cluster **5** shows a substantial shift of its *N*-Me signal; the dithiocarbamate ligand presumably assumes the bidentate (possibly unsymmetrical) coordination proven by X-ray analysis of [Fe<sub>4</sub>S<sub>4</sub>(SPh)<sub>2</sub>(S<sub>2</sub>CNEt<sub>2</sub>)<sub>2</sub>]<sup>2-</sup> and [Fe<sub>4</sub>S<sub>4</sub>Cl<sub>4-n</sub>(S<sub>2</sub>CNEt<sub>2</sub>)<sub>n</sub>]<sup>2-</sup> (*n* = 1, 2),<sup>18</sup> in which the mean ligand bite distance is 2.87 (2) Å. The bidentate nature of the py-2-S<sup>-</sup> ligand in **6** is shown by substantial negative shifts of three of the four protons (Figure 5). Binding through sulfur only would be expected to produce the sign alternation observed with **4**. Further, the small N-S bite distance should promote bidentate coordination, as found in [Fe(py-2-S)<sub>3</sub>]<sup>-</sup>,<sup>36</sup> where the mean values of this distance and the N-Fe-S angles are 2.602 (2) Å and 66.1 (2)°, respectively. Tridentate binding of tacn and Me<sub>3</sub>tacn to Fe(II,III) in [Fe(tacn)]<sup>2+</sup>,<sup>3+37</sup> and other species<sup>38,39</sup> is well established. The two negatively shifted C-H resonances of cluster **8** (spectrum not shown) are consistent with a tridentate tacn ligand and averaging of members of two pairs of inequivalent axial and equatorial protons in the skew conformation of the five-membered chelate rings. Among the numerous complexes of tacn,<sup>38</sup> the conformation in question is illustrated by trigonally symmetric [(tacn)ReO<sub>3</sub>]<sup>+</sup> in the crystalline state.<sup>40</sup> Similarly, the crystallographically demonstrated tridentate coordination of

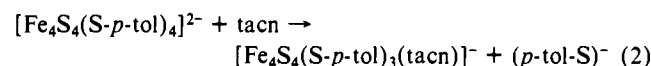
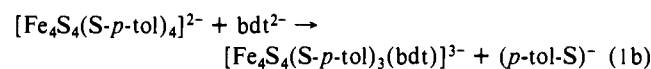
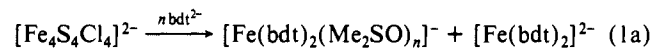
Table III. <sup>1</sup>H Chemical Shifts of [Fe<sub>4</sub>S<sub>4</sub>L<sub>3</sub>L']<sup>2-</sup> Clusters in Me<sub>2</sub>SO-*d*<sub>6</sub> at 297 K

| cluster   | shifts, ppm |             |              |  |
|---|-------------|-------------|--------------|--|
|   | <i>o</i> -H | <i>m</i> -H | <i>p</i> -Me | L'   |
| [Fe <sub>4</sub> S <sub>4</sub> (S- <i>p</i> -tol) <sub>3</sub> (tacn)] <sup>-</sup>                  | 5.6 (br)    | 8.18        | 4.28         | 8.3 (v br), 12.2                               |
| [Fe <sub>4</sub> S <sub>4</sub> (S- <i>p</i> -tol) <sub>3</sub> (HB(pz) <sub>3</sub> )] <sup>2-</sup> | 4.96        | 8.32        | 4.53         | 11.1, 11.7                                     |
| [Fe <sub>4</sub> S <sub>4</sub> Cl <sub>3</sub> (HB(pz) <sub>3</sub> )] <sup>2-</sup>                 |             |             |              | 11.8, 12.1                                     |
| [Fe <sub>4</sub> S <sub>4</sub> (S- <i>p</i> -tol) <sub>3</sub> (bdt)] <sup>3-</sup>                  | 5.32        | 8.07        | 4.15         | 7.10 (H <sub>b</sub> ), 9.83 (H <sub>a</sub> ) |
| [Fe <sub>4</sub> S <sub>4</sub> (S- <i>p</i> -tol) <sub>4</sub> ] <sup>2-</sup>                       | 5.63        | 7.96        | 3.95         |  |

[HB(pz)<sub>3</sub>]<sup>-</sup> to Fe(II,III) centers<sup>41,42</sup> provides support for the formulation of clusters **7a** and **9**. The spectrum of **9** (Figure 6) contains two sharp pyrazolyl ring resonances with negative shifts; it is likely that 3-H is paramagnetically broadened beyond detection. The considerable differences in isotropic shifts of these two clusters argue against a static bidentate coordination by [HB(pz)<sub>3</sub>]<sup>-</sup> in the latter. Lastly, in all of their structurally characterized complexes, tacn and [HB(pz)<sub>3</sub>]<sup>-</sup> function exclusively as tridentate ligands.

Clusters **10–14** have effective trigonal symmetry in solution, indicating stereochemical nonrigidity of the bidentate ligand at the unique subsite. That the ligands are bidentate is indicated by the presence of two bdt and two Me<sub>4</sub>bdt resonances in **11** and **14**, respectively. For all clusters in the set, signals of substituents ortho to oxygen and sulfur atoms were identified by line width. The spectrum of **10** (Figure 7) was assigned under the assumption that, as with **3** and **4**, delocalization through the oxygen atom pathway predominates. The spectra do not show the alternating signs of isotropic shifts observed for **3**, **4**, and [Fe<sub>4</sub>S<sub>4</sub>L<sub>4</sub>]<sup>2-</sup> (L = *o*-C<sub>6</sub>H<sub>4</sub>(OH)S<sup>-</sup>, *o*-C<sub>6</sub>H<sub>4</sub>(SMe)S<sup>-</sup>),<sup>17</sup> as would be expected if any ligands were adventitiously monoprotonated. The spectrum of **13** (Figure 8) demonstrates this point. Shifts of the resonances of H<sub>a,c</sub> protons necessarily ortho and meta to either sulfur atom, are both negative. It is concluded that clusters **10–14** have a unique five-coordinate subsite.

**Factors Promoting the Formation and Stabilization of Substituted Clusters.** In earlier reports of the substitution reactions of **1**, we have shown that the trithiolate ligand LS<sub>3</sub> supports site-specific reactions by directing kinetic reactivity to a single subsite with a good leaving group.<sup>2</sup> Core stability of the reaction products [Fe<sub>4</sub>S<sub>4</sub>(LS<sub>3</sub>)L']<sup>2-</sup> was not in question, given the stability of the conventional clusters [Fe<sub>4</sub>S<sub>4</sub>L'<sub>4</sub>]<sup>2-</sup> (L' = Cl<sup>-</sup>, RS<sup>-</sup>, ArO<sup>-</sup>). Clusters **3** and **4** fall into this category. Of the remaining clusters (Figure 2), only **5** contains a ligand previously bound to a [Fe<sub>4</sub>S<sub>4</sub>]<sup>2+</sup> core. Reaction of [Fe<sub>4</sub>S<sub>4</sub>Cl<sub>4</sub>]<sup>2-</sup> with NaS<sub>2</sub>CNEt<sub>2</sub> yields [Fe<sub>4</sub>S<sub>4</sub>Cl<sub>4-n</sub>(S<sub>2</sub>CNEt<sub>2</sub>)<sub>n</sub>]<sup>2-</sup> (*n* = 1, 2).<sup>18</sup> Consequently, the core of **5** requires no special stabilization. However, this is not necessarily true for other clusters in Figure 2, the possible role of the LS<sub>3</sub> ligand being both kinetic and thermodynamic. To explore the factors affecting the formation and stability of selected substituted clusters, reactions **1–3** and several others were examined in Me<sub>2</sub>SO solutions. These reactions employ as starting materials clusters with viable leaving groups of different labilities (Cl<sup>-</sup> > ArS<sup>-</sup>) in a polar solvent such as Me<sub>2</sub>SO. Cluster reaction products were identified from their <sup>1</sup>H NMR chemical shifts, listed in Table III, which compare closely with those of the corresponding clusters [Fe<sub>4</sub>S<sub>4</sub>(LS<sub>3</sub>)L']<sup>2-</sup>. Free *p*-tolylthiolate was readily detected by its resonances at 2.04, 6.46, and 6.87 ppm.



(41) Oliver, J. D.; Mullica, D. F.; Hutchinson, B. B.; Milligan, W. O. *Inorg. Chem.* **1980**, *19*, 165.

(42) (a) Armstrong, W. H.; Spool, A.; Papaefthymiou, G. C.; Frankel, R. B.; Lippard, S. J. *J. Am. Chem. Soc.* **1984**, *106*, 3653. (b) Armstrong, W. H.; Lippard, S. J. *J. Am. Chem. Soc.* **1984**, *106*, 4632.

(35) Use of ligand anion shifts is dictated by the insolubility of certain protonated ligands, among them L(SH)<sub>3</sub>, in Me<sub>2</sub>SO. Isotropic shifts are used here only in a comparative sense. Signals of 2-H are paramagnetically broadened and in some cases were not located. They are omitted from Table I, as are the relatively small and less informative isotropic shifts of the *p*-tolylthio groups of LS<sub>3</sub>. Note that definite assignment of ligand (L') resonances in **6**, **7ab**, and **9** were not made.

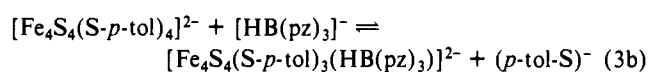
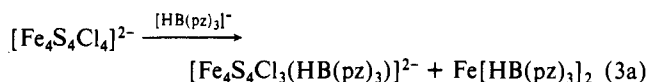
(36) Rosenfield, S. G.; Swedberg, S. A.; Arora, S. K.; Mascharak, P. K. *Inorg. Chem.* **1986**, *25*, 2109.

(37) Boeyens, J. C. A.; Forbes, A. G. S.; Hancock, R. D.; Wiegardt, K. *Inorg. Chem.* **1985**, *24*, 2926.

(38) Chaudhuri, P.; Wiegardt, K. *Prog. Inorg. Chem.* **1987**, *35*, 329.

(39) (a) Wiegardt, K.; Pohl, K.; Gebert, W. *Angew. Chem., Int. Ed. Engl.* **1983**, *22*, 727. (b) Spool, A.; Williams, I. D.; Lippard, S. J. *Inorg. Chem.* **1985**, *24*, 2156. (c) Chaudhuri, P.; Wiegardt, K.; Nuber, B.; Weiss, J. *Angew. Chem., Int. Ed. Engl.* **1985**, *24*, 778. (d) Hartman, J. R.; Rardin, R. L.; Chaudhuri, P.; Pohl, K.; Wiegardt, K.; Nuber, B.; Weiss, J.; Papaefthymiou, G. C.; Frankel, R. B.; Lippard, S. J. *J. Am. Chem. Soc.* **1987**, *109*, 7387. (e) Wiegardt, K.; Pohl, K.; Bossek, U.; Nuber, B.; Weiss, J. Z. *Naturforsch.* **1988**, *43b*, 1184.

(40) Wiegardt, K.; Pomp, C.; Nuber, B.; Weiss, J. *Inorg. Chem.* **1986**, *25*, 1659.



Shown in Figure 9 are  $^1\text{H}$  NMR spectra of the products of reaction 1a with 1, 2, and 4 equiv of  $\text{Na}_2\text{bdt}$ . At  $n = 1$  and 2, two signals at 11.0 and  $-9.60$  (pair A) and two others at  $-29.4$  and  $-34.0$  (pair B) appear. Pair B arises from  $[\text{Fe}(\text{bdt})_2(\text{Me}_2\text{SO})_n]^-$  as shown by measurement of a  $\text{Me}_2\text{SO}$  solution prepared from authentic  $(\text{Et}_4\text{N})_2[\text{Fe}_2(\text{bdt})_4]^{2-}$ .<sup>26</sup> At  $n = 4$ , the intensity of pair B decreases and pair A is replaced by resonances at 11.71 and  $-9.77$  (pair C). The signals of pair C are the same as those of the reaction product of  $\text{FeCl}_2 + 2\text{Na}_2\text{bdt}$ , which in turn are identical with those of authentic  $(\text{Ph}_4\text{As})_3[\text{Fe}(\text{bdt})_2]^{4-}$  in  $\text{Me}_2\text{SO}$  solution. The reduction of Fe(III) to Fe(II) is caused by dithiolate or sulfide. In contrast to this rather complicated reaction system, reaction 1b proceeds to completion immediately but does also form  $[\text{Fe}(\text{bdt})_2(\text{Me}_2\text{SO})_n]^-$  as a minority product. Reaction of  $[\text{Fe}_4\text{S}_4\text{Cl}_4]^{2-}$  with 1 equiv of tacn leads to the immediate separation of a black intractable solid, the amount of which increases with increasing equivalents of tacn. Reaction 2, however, results in at least 50% formation of substituted cluster within 30 min. With 2–4 equiv of tacn, there is clear NMR evidence for incomplete formation of a disubstituted cluster, but a black precipitate appears when about 4 equiv of ligand have been added.

Reaction 3a produces a mixture of monosubstituted cluster and, as the major product,  $\text{Fe}[\text{HB}(\text{pz})_3]_2$ , which exists in a spin equilibrium in solution.<sup>44</sup> Further stepwise addition of up to 4 equiv of ligand increased the ratio of cluster to mononuclear complex slightly. Reaction 3b is a clean equilibrium in which there is 35% monosubstituted cluster formation with 1 equiv of ligand and 90% with 4 equiv.

The foregoing results show that **8** and **11** (and presumably other type **2** clusters) owe their stability primarily to the presence of terminal thiolate ligands. In these cases, there is no indication of stability of monosubstituted clusters with chloride terminal ligands. A cluster containing one  $[\text{HB}(\text{pz})_3]^-$  ligand can abide chloride ligands, but the absence of an Fe-containing byproduct in reaction 3b again emphasizes the stabilizing role of terminal thiolates. Thus the principal attribute of the  $\text{LS}_3$  ligand as expressed in the reactions of **1** is kinetic. *Cluster 1 offers the advantage of rapid, stoichiometric subsite-specific reactions with, usually, minimal or no byproducts.* While a similar conclusion was drawn earlier,<sup>2</sup> it is now seen to apply to a much larger variety of ligands, including a number of others to be reported subsequently.<sup>45</sup>

With the identification of clusters in hand, we turn to an examination of two properties potentially susceptible to modulation by ligand variation at a single subsite. These are relative stabilities of oxidation states and electron distribution as sensed by  $^{57}\text{Fe}$  Mössbauer spectroscopy. Both of these properties are intimately connected with the biological function of  $\text{Fe}_4\text{S}_4$  clusters. Owing to the lack of suitable compounds, the effects of single subsite variation on these properties is heretofore unknown.

**Relative Stabilities of Oxidation States.** The electron-transfer reactions of native and synthetic  $\text{Fe}_4\text{S}_4$  clusters are summarized in Figure 10. The  $[\text{Fe}_4\text{S}_4]^{0/1+}$  state has not been proven in a protein. The  $[\text{Fe}_4\text{S}_4]^{2+/+}$  ( $\text{Fd}_{\text{ox/red}}$ ) couple is the most prevalent biologically. The  $[\text{Fe}_4\text{S}_4]^{3+/2+}$  ( $\text{HP}_{\text{ox/red}}$ ) couple is restricted to a subclass of ferredoxins, the "high-potential" proteins. Approximate ranges of native cluster potentials are indicated. As far as is known, these potentials refer to  $\text{Fe}_4\text{S}_4(\text{S-Cys})_4$  clusters, i.e., those with tetrahedral subsites and exclusive cysteinate ligation. Analogue clusters

(43) Sellman, D.; Kleine-Kleffmann, U.; Zapf, L.; Huttner, G.; Zsolnai, L. *J. Organomet. Chem.* **1984**, 263, 321. In this reference, the anion is shown to be planar in the solid state.

(44) Jesson, J. P.; Trofimenko, S.; Eaton, D. R. *J. Am. Chem. Soc.* **1967**, 89, 3158. In  $\text{Me}_2\text{SO}$  at 297 K, the complex is characterized by signals at 16.2, 8.30, and 6.5 (br) ppm.

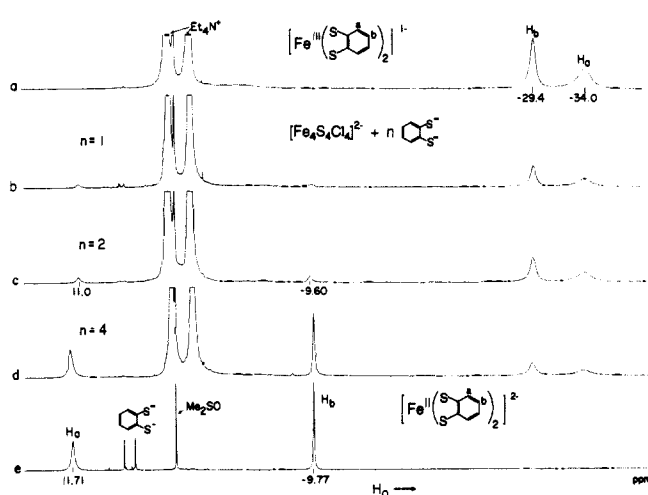


Figure 9.  $^1\text{H}$  NMR spectra in  $\text{Me}_2\text{SO}-d_6$  at 297 K: (a) authentic  $(\text{Et}_4\text{N})[\text{Fe}(\text{bdt})_2(\text{Me}_2\text{SO})_n]^-$ ; (b–d) reaction products of  $[\text{Fe}_4\text{S}_4\text{Cl}_4]^{2-}$  with 1, 2, and 4 equiv of  $\text{Na}_2(\text{bdt})$ ; and (e)  $[\text{Fe}(\text{bdt})_2]^{2-}$ , generated in situ by the reaction of  $\text{FeCl}_2$  with a small excess of  $\text{Na}_2(\text{bdt})$ . Signal assignments are indicated.

#### ELECTRON TRANSFER SERIES OF $[\text{Fe}_4\text{S}_4]$ CLUSTERS

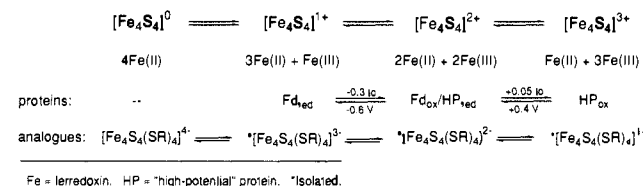


Figure 10. Electron-transfer series of  $\text{Fe}_4\text{S}_4$  protein clusters and their synthetic analogues, showing core charges and formal oxidation states and approximate ranges of protein potentials  $E_0'$ .

exhibit two or all three redox steps. Their potentials are dependent on the substituents R, which are readily changed only in sets of four. Inasmuch as detection of different ligation modes may eventuate for protein-bound  $\text{Fe}_4\text{S}_4$  clusters,<sup>46</sup> the question arises as to how the relative stabilities of core oxidation states are affected by different patterns of ligation. With access to the clusters of Figure 2, this matter can be addressed in terms of variant ligation at a single subsite. With very few exceptions,<sup>18,48</sup> changes in the oxidation state stabilities have been examined only by variation of the entire ligand set. Analogue potentials of interest here are  $[\text{Fe}_4\text{S}_4]^{2+/+}$  and, particularly,  $[\text{Fe}_4\text{S}_4]^{3+/2+}$ . Values are compiled in Table II. Representative cyclic voltammograms are shown in Figures 11 and 12.

(a)  $[\text{Fe}_4\text{S}_4]^{2+/+}$ . Reductions of the dinegative clusters **5** and **9** occur at potentials more negative than those of **1** and **4** as references. At equal cluster charge, the potentials reflect increased core electron density effected by the bi- and tridentate ligands. An exception is **6**, where the effect of nitrogen coordination on potentials vs those of **4** is essentially nil. Similarly, the potentials of trinegative clusters **10–14** are 290–450 mV more negative in  $\text{Me}_2\text{SO}$  than that of the reference **4**. These shifts are due to the combined effects of increased cluster charge and core electron density introduced by the dinegative chelate ligands. As would be expected from substituent effects, the potential of cluster **14** is the most negative.

(45) Weigel, J. A.; Holm, R. H. Results to be published.

(46) The best characterized case of native Fe–S clusters with non-cysteinate ligands is the Reiske proteins, which have  $\text{Fe}_2\text{S}_2(\text{S-Cys})_2(\text{N-His})_2$  sites. Their  $[\text{Fe}_2\text{S}_2]^{2+/1+}$  potentials are some 250–750 mV higher than those of conventional  $\text{Fe}_2\text{S}_2(\text{S-Cys})_2$  sites.

(47) (a) Kuila, D.; Fee, J. A.; Schoonover, J. R.; Batie, C. J.; Ballou, D. P. *J. Am. Chem. Soc.* **1987**, 109, 1559. (b) Gurbiel, R. J.; Batie, C. J.; Sivaraja, M.; True, A. E.; Fee, J. A.; Hoffman, B. M.; Ballou, D. P. *Biochemistry* **1989**, 28, 4861.

(48) Johnson, R. W.; Holm, R. H. *J. Am. Chem. Soc.* **1978**, 100, 5338.



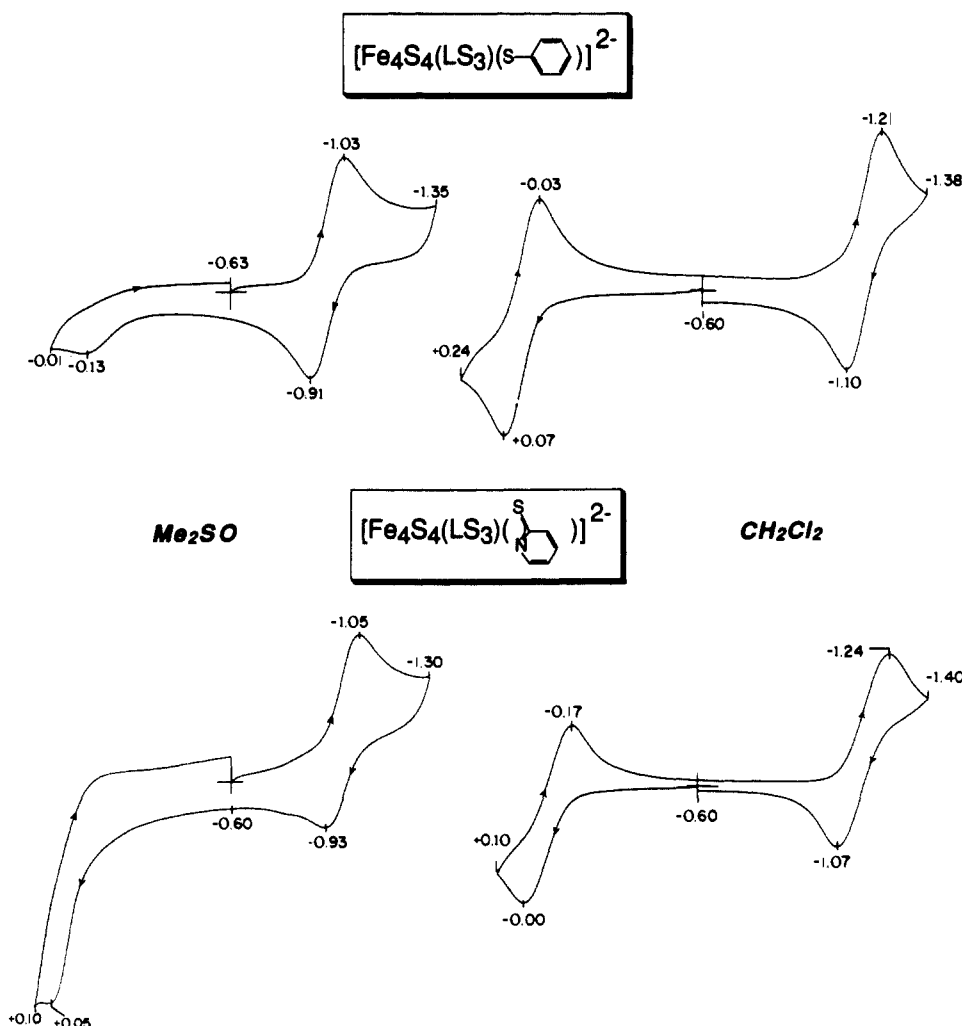


Figure 11. Cyclic voltammograms (50 mV/s) of clusters 4 (upper) and 6 (lower) in  $\text{Me}_2\text{SO}$  and dichloromethane solutions; peak potentials are indicated.

Cluster charge does not necessarily produce potential shifts in the anticipated direction. Uninegative cluster 8 might be expected to reduce at a more positive potential than any dinegative cluster in Table II. While this is the case for 8 vs 5 and 9, it does not hold with regard to 1, 4, and 6. The shift vs 4, for example, is  $-160$  mV in  $\text{Me}_2\text{SO}$  and  $-70$  mV in dichloromethane. The positive potential shift foreseen on a charge basis alone is evidently overcompensated by electron donation to the core by the three nitrogen atoms of the tacn ligand.

(b)  $[\text{Fe}_4\text{S}_4]^{3+/2+}$ . Most analogue clusters  $[\text{Fe}_4\text{S}_4(\text{SR})_4]^{2-}$  show grossly irreversible oxidations in polar solvents. However, R substituents with one or both of the properties of steric bulk and hydrophobicity can lead to reversible couples.<sup>49-53</sup> One such oxidized cluster has been isolated.<sup>51</sup> Irreversible behavior extends to the majority of dinegative clusters examined here, including 4 and 6 as shown in Figure 11. However, without exception the bidentate ligated clusters 10-14 exhibit chemically reversible oxidations at  $-0.43$  to  $-0.75$  V in  $\text{Me}_2\text{SO}$ , a property illustrated for three clusters in Figure 12. For cluster 13 in  $\text{Me}_2\text{SO}$ , coulometric oxidation followed by reduction over 45 min to 1 h for each step gave  $n = 0.95 e^-$  and  $0.90 e^-$ , respectively. Estimating the oxidation potential of reference cluster 4 as  $-0.1$  V in  $\text{Me}_2\text{SO}$ ,

the potential is shifted by about  $-520$  mV with 11. The order of potentials is again consistent with expected substituent effects, the most negative potential ( $-0.75$  V) being found with 14. The causes of these potential shifts with 11 and related clusters are of course the same as those displacing  $[\text{Fe}_4\text{S}_4]^{2+/+}$  potentials in the cathodic direction, but the effect is larger. The consequences of these shifts are to stabilize the  $[\text{Fe}_4\text{S}_4]^{3+/2+}$  oxidation levels toward reduction relative to a suitable reference, as in the particularly appropriate comparison of 11 vs 4.

In a related observation,<sup>54</sup> the potential for the  $[\text{VFe}_3\text{S}_4(\text{LS}_3)(\text{CN})_3]^{3-/4-}$  couple is 490 mV more negative than is that for the isoelectronic couple  $[\text{VFe}_3\text{S}_4(\text{LS}_3)(\text{Me}_2\text{SO})_3]^{0/-}$ . The potential shift is comparable to the difference between 13 and 4, but the charge differs by three units instead of one.

All clusters of the type  $[\text{Fe}_4\text{S}_4(\text{LS}_3)\text{L}]^{2-}$  that have been tested by cyclic voltammetry show chemically reversible reductions and oxidations in dichloromethane. This behavior is contrasted with that in  $\text{Me}_2\text{SO}$  for clusters 4 and 6 in Figure 11 and renders the  $[\text{Fe}_4\text{S}_4]^{3+}$  oxidation state potentially accessible for study in a number of clusters.

**Modulation of Electron Distribution.** To investigate any effects of this type, eight clusters were examined by Mössbauer spectroscopy. Spectra are presented in Figure 13 and isomer shifts ( $\delta$ ), quadrupole splittings ( $\Delta E_Q$ ), and line widths ( $\Gamma$ ) resulting from least-squares fits are listed in Table IV. Spectra were analyzed by requiring that the quadrupole doublet arising from the unique subsite account for 25% of the total absorption. Inasmuch as the majority of the clusters have at most mirror symmetry, two other doublets were included with unconstrained in-

(49) Mascharak, P. K.; Hagen, K. S.; Spence, J. T.; Holm, R. H. *Inorg. Chim. Acta* **1983**, *80*, 157.

(50) Ueyama, N.; Terakawa, T.; Sugawara, T.; Fuji, M.; Nakamura, A. *Chem. Lett.* **1984**, 1287.

(51) O'Sullivan, T.; Millar, M. M. *J. Am. Chem. Soc.* **1985**, *107*, 4096.

(52) Okuno, Y.; Uoto, K.; Yonemitsu, O.; Tomohiro, T. *J. Chem. Soc., Chem. Commun.* **1987**, 1018.

(53) Nakamoto, M.; Tanaka, K.; Tanaka, T. *J. Chem. Soc., Chem. Commun.* **1988**, 1422.

(54) Ciurli, S.; Holm, R. H. *Inorg. Chem.* **1989**, *28*, 1685.



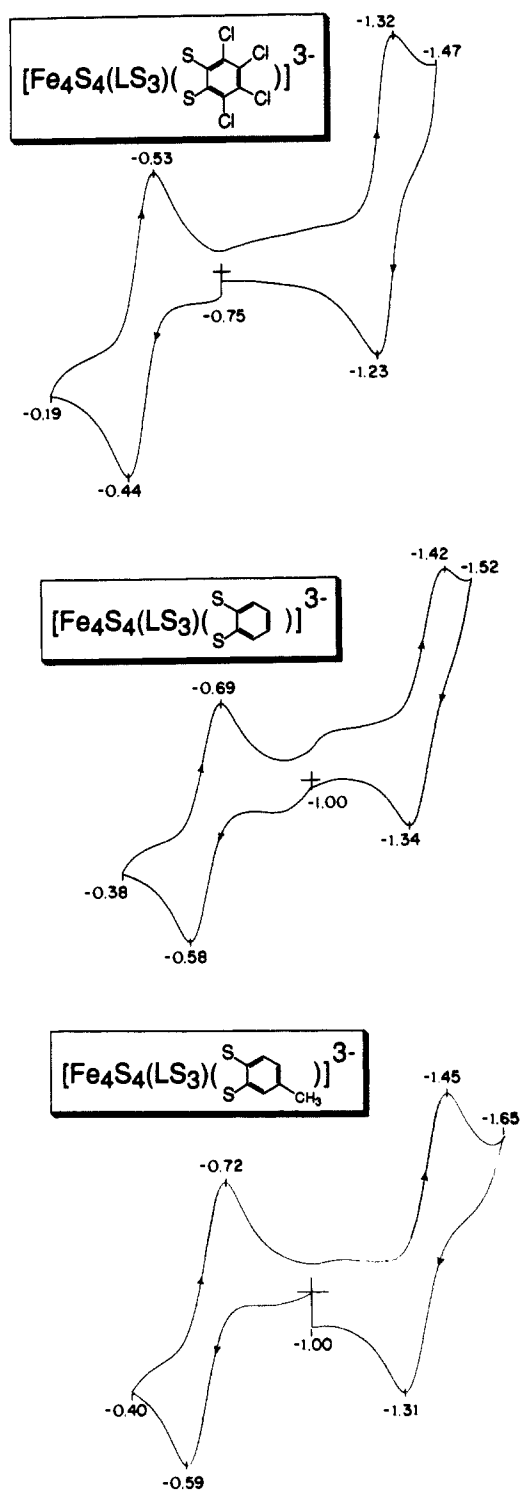


Figure 12. Cyclic voltammograms (50 mV/s) of clusters **12**, **11**, and **13** (descending order) in  $\text{Me}_2\text{SO}$  solutions; peak potentials are indicated.

tensities. Line widths were also unconstrained. The higher velocity component of the unique subsite doublet is usually discernible in the spectra, and in two cases (**7a**, **9**) it is resolved.

Clusters of the type  $[\text{Fe}_4\text{S}_4(\text{SR})_4]^{2-}$  exhibit Mössbauer spectra at 4.2 K that consist of a single symmetrical quadrupole doublet.<sup>55,56</sup> At this temperature,  $(\text{Et}_4\text{N})_2[\text{Fe}_4\text{S}_4(\text{SPh})_4]$  has  $\delta = 0.35$  mm/s and  $\Delta E_Q = 1.10$  mm/s.<sup>55</sup> Cluster **4** has nearly the same parameters except at the unique subsite, where the apparent quadrupole splitting is larger. Relative to **4**, increase of coord-

Table IV. Mössbauer Spectral Properties of  $[\text{Fe}_4\text{S}_4(\text{LS}_3)\text{L}]^{2-}$  Clusters at 4.2 K

| cluster   | L' | $\delta$ , <sup>a</sup> mm/s | $\Delta E_Q$ , mm/s | $\Gamma$ , mm/s | % A <sup>b</sup> |
|-----------|----|------------------------------|---------------------|-----------------|------------------|
| <b>4</b>  |    | 0.34 (A)                     | 1.40                | 0.27            | 25               |
|           |    | 0.34 (B)                     | 1.04                | 0.41            | 75               |
| <b>5</b>  |    | 0.55 (A)                     | 1.85                | 0.52            | 25               |
|           |    | 0.34 (B)                     | 0.93                | 0.31            | 37               |
|           |    | 0.35 (C)                     | 1.28                | 0.32            | 38               |
| <b>6</b>  |    | 0.52 (A)                     | 1.70                | 0.56            | 25               |
|           |    | 0.34 (B)                     | 0.94                | 0.30            | 39               |
|           |    | 0.34 (C)                     | 1.26                | 0.29            | 36               |
| <b>7a</b> |    | 0.83 (A)                     | 2.38                | 0.62            | 25               |
|           |    | 0.26 (B)                     | 0.62                | 0.50            | 20               |
|           |    | 0.35 (C)                     | 1.10                | 0.40            | 55               |
| <b>8</b>  |    | 0.68 (A)                     | 1.55                | 0.36            | 25               |
|           |    | 0.32 (B)                     | 0.96                | 0.33            | 37               |
|           |    | 0.34 (C)                     | 1.28                | 0.32            | 38               |
| <b>9</b>  |    | 0.79 (A)                     | 2.03                | 0.38            | 25               |
|           |    | 0.31 (B)                     | 0.84                | 0.30            | 34               |
|           |    | 0.34 (C)                     | 1.23                | 0.33            | 41               |
| <b>10</b> |    | 0.52 (A)                     | 1.47                | 0.46            | 25               |
|           |    | 0.34 (B)                     | 1.03                | 0.34            | 43               |
|           |    | 0.33 (C)                     | 1.37                | 0.29            | 32               |
| <b>13</b> |    | 0.52 (A)                     | 1.97                | 0.48            | 25               |
|           |    | 0.37 (B)                     | 0.96                | 0.30            | 40               |
|           |    | 0.36 (C)                     | 1.29                | 0.28            | 35               |

<sup>a</sup>Relative to Fe metal at 4.2 K; to convert to values at 298 K vs Fe metal add 0.12 mm/s. <sup>b</sup>Percent of total absorption.

dination number at that subsite increases the isomer shifts in all clusters by ca. 0.2 mm/s or more and (excluding **10**) increases the quadrupole splittings by at least 0.15 mm/s. For the present set of clusters and those examined earlier<sup>17,18</sup> whose five-coordinate subsite contains one anionic sulfur ligand, the parameter ranges are relatively narrow:  $\delta = 0.51$ – $0.55$  and  $\Delta E_Q = 1.5$ – $2.0$  mm/s. For six-coordinate clusters **8** and **9**,  $\delta$  values are much higher (0.68, 0.79 mm/s) but quadrupole splittings are in the previous range.

Mössbauer parameters of the unique subsites cannot be closely interpreted in terms of oxidation state, owing to the absence of well-defined reference compounds. However, in terms of isomer shifts for diverse sets of high-spin Fe(II,III) complexes,<sup>57</sup> values for **5**, **6**, **10**, and **13** tend toward Fe(III) and those for **7a**, **8**, and **9** toward Fe(II). At least for dithiocarbamate and bdt-type ligands, this is consistent with the usual tendencies of oxidation state stabilization. Inasmuch as the isomer shifts of tetrahedral  $\text{FeS}_4$  sites are linearly related to (mean) oxidation state,<sup>58</sup> it might be expected that the shifts of the three other subsites would reflect the charge bias at the unique subsite. The only  $[\text{Fe}_4\text{S}_4]^{2+}$  clusters with a valence-localized subsite are  $[\text{Fe}_4\text{S}_4(\text{LS}_3)(\text{RNC})_3]^{2-}$ , which contain low-spin Fe(II).<sup>16</sup> For the non-unique subsites of the R = *t*-Bu cluster,  $\delta_{\text{av}} = 0.30$  mm/s. This corresponds exactly to the shift predicted by the empirical relationship between  $\delta$  and oxidation state for  $\text{Fe}^{2.67+}$ .<sup>58</sup> In the absence of complete localization, deviations from  $\delta = 0.36$  mm/s for  $\text{Fe}^{2.5+}$  subsites of a  $[\text{Fe}_4\text{S}_4]^{2+}$  core will be smaller. While there are trends consistent with oxidation state bias at the unique site (e.g., **7a**, **8**, **9**, **13**), the collective data indicate the absence of valence localization in the clusters of Table IV.

**Summary.** The following are the principal findings and conclusions of this investigation.

(1) Cluster **1** undergoes rapid and usually stoichiometric subsite-specific substitution reactions with a variety of bidentate and

(57) Greenwood, N. N.; Gibb, T. C. *Mössbauer Spectroscopy*; Chapman and Hall Ltd.: London, 1971; Chapter 6.

(58) Christou, G.; Mascharak, P. K.; Armstrong, W. H.; Papaefthymiou, G. C.; Frankel, R. B.; Holm, R. H. *J. Am. Chem. Soc.* **1982**, *104*, 2820. For tetrahedral  $\text{FeS}_4$  sites at 4.2 K,  $\delta = 1.44 - 0.43s$ , where  $s$  is the Fe (mean) oxidation state.

(55) Frankel, R. B.; Averill, B. A.; Holm, R. H. *J. Phys. (Paris)* **1974**, *35*, C6-107.

(56) Kanatzidis, M. G.; Baenziger, N. C.; Coucouvanis, D.; Simopoulos, A.; Kostikas, A. *J. Am. Chem. Soc.* **1984**, *106*, 4500.

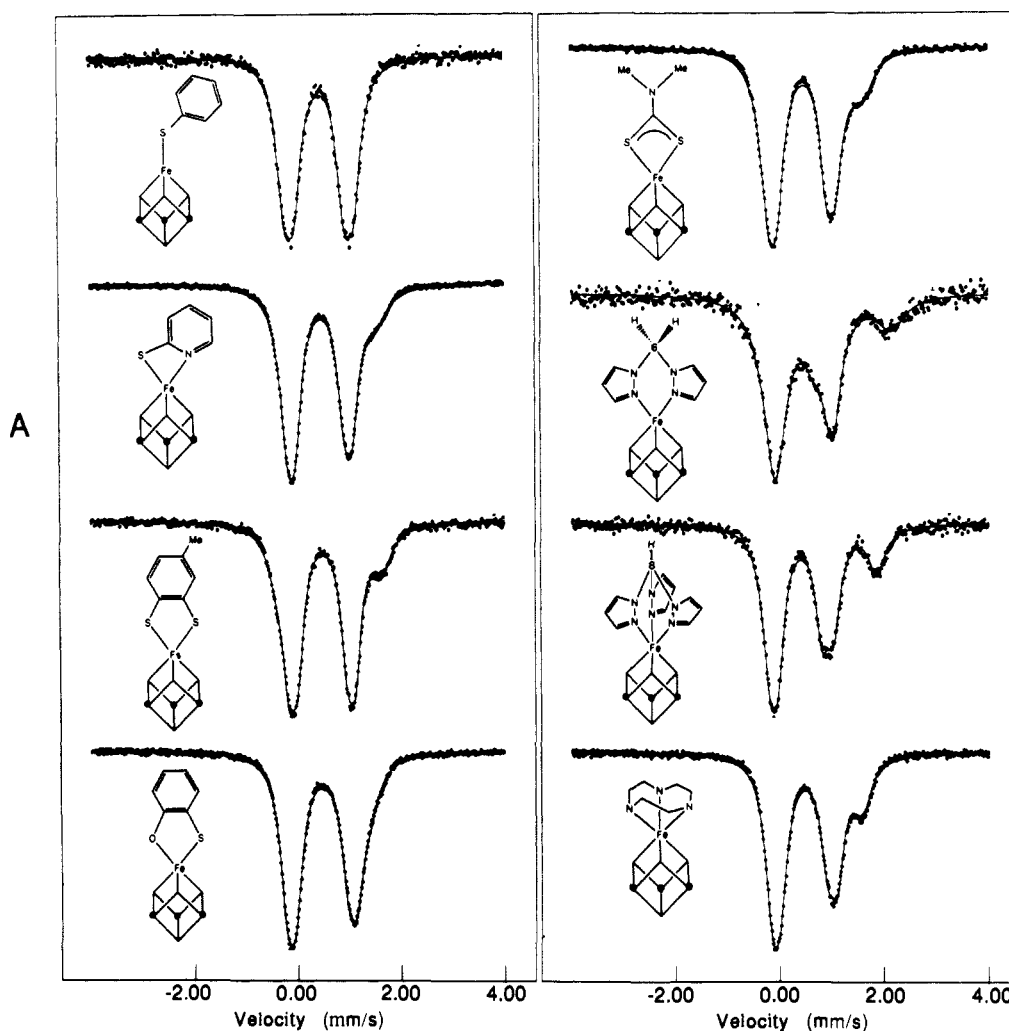


Figure 13. Mössbauer spectra (descending order) of clusters 4, 6, 13, 10 (left) and 5, 7a, 9, 8 (right) at 4.2 K.

tridentate ligands  $L'$  to form the species  $[\text{Fe}_4\text{S}_4(\text{LS}_3)L']^{2-}$  (5–14), thereby broadening the scope of such reactions beyond unidentate ligands.

(2) Reaction products have effective trigonal symmetry in solution (NMR criterion) and are detectable because of the extreme sensitivity of isotropic (contact) shifts of 4-Me, 5-H, and 6-Me of ligand  $\text{LS}_3$  to the identity of  $L'$ , and by the isotropic shifts of  $L'$  itself.

(3) Stabilities of substituted clusters 8 and 11 (and others of type 2) derive mainly from the presence of thiolate ligands at the other three subsites rather than from any securing structural feature of the  $\text{LS}_3$  ligand. While the clusters  $[\text{Fe}_4\text{S}_4(\text{LS}_3)L']^{2-}$  need not necessarily be formed as in (1), the advantage of cluster 1 is the predictable occurrence of rapid subsite-specific reactions with minimal byproducts.

(4) Clusters containing dinegative bidentate ligands (10–14) exhibit chemically reversible  $[\text{Fe}_4\text{S}_4]^{3+/2+}$  couples in  $\text{Me}_2\text{SO}$  at potentials ca. 300 to 700 mV more negative than that of reference cluster 4. Potentials of the  $[\text{Fe}_4\text{S}_4]^{2+/+}$  couples are shifted to more negative values by 290–450 mV. While the effects of cluster charge and core electron density are not strictly separable, substituent effects on potentials for 11–14 (270-mV range), reduction of mononegative cluster 8 at a more negative potential than 1 and 4 (by 230 and 100 mV, respectively), and previous observations of the ligand dependence of  $[\text{VFe}_3\text{S}_4]^{2+/+}$  potentials<sup>54</sup> make clearly evident the operation of the latter factor.

(5) Core charge distributions are measurably influenced by substitution, with isomer shifts indicating subsites with more "ferric-like" character in 5, 6, 11, and 13 relative to the more "ferrous-like" character in 7a, 8, and 9. Isomer shifts of the remaining three subsites do not indicate the existence of valence

localization at the unique subsite.

**Possible Biological Implications.** For all but one native  $\text{Fe}_4\text{S}_4$  cluster, the proven terminal ligation is by cysteinate residues, leading to the tetrahedral subsites in  $\text{Fe}_4\text{S}_4(\text{S-Cys})_4$ . Proof follows from protein crystallography<sup>59</sup> and in one case from detailed analysis of protein primary structure.<sup>60</sup> The exception is the active form of aconitase, in which three subsites are bound by cysteinate and the other contains a water or hydroxide as the terminal ligand.<sup>7</sup> A noteworthy result of the present work is the preparation of clusters with subsite coordination numbers of 5 and 6. While these arrangements have been accomplished only with chelating ligands, the possibility remains that protein structure could impose five- or six-coordination at a cluster subsite. If, for example, the pyrazolylborate ligands in 7a and 9 and the bdt ligand in 11 are accepted as reasonable simulators of coordination by imidazole and cysteinate, respectively, the data in Tables II and IV approximate the intrinsic effects on redox potentials<sup>61</sup> and Mössbauer

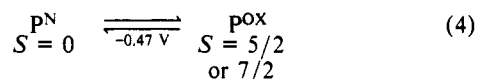
(59) (a) Adman, E. T.; Sieker, L. C.; Jensen, L. H. *J. Biol. Chem.* **1973**, *248*, 3987. (b) Carter, C. W., Jr.; Kraut, J.; Freer, S. T.; Alden, R. A. *J. Biol. Chem.* **1974**, *249*, 6339. (c) Stout, G. H.; Turley, S.; Sieker, L. C.; Jensen, L. H. *Proc. Natl. Acad. Sci. U.S.A.* **1988**, *85*, 1020. (d) Stout, C. D. *J. Biol. Chem.* **1988**, *263*, 9256; *J. Mol. Biol.* **1989**, *205*, 545. (e) Fukuyama, K.; Nagahara, Y.; Tsukihara, T.; Katsube, Y.; Hase, T.; Matsubara, H. *J. Mol. Biol.* **1988**, *199*, 183.

(60) Howard, J. B.; Davis, R.; Moldenhauer, B.; Cash, V. L.; Dean, D. J. *Biol. Chem.* **1989**, *264*, 11270.

(61) We place a minor caveat on the role of bidentate ligands like bdt on potentials inasmuch as we do not know if chelate ring formation, relative to two separate thiolate ligands, leads to a preferential or otherwise unequal stabilization of one or both oxidation states. We have never been able to prepare stable clusters with two thiolate ligands on the same subsite, presumably because of size effects and charge repulsion. Use of the 1,2-ethanedithiolate ligand leads to formation of a bridged double cubane cluster.<sup>15</sup>

spectral parameters by these ligand sets at a single subsite.

Of all native clusters, the "P-clusters" of nitrogenase are the best candidates for non-cysteinate or otherwise unconventional terminal ligation. Their properties, which are consistent with but do not necessarily prove the  $\text{Fe}_4\text{S}_4$  cubane-type formulation, are summarized elsewhere.<sup>12,62</sup> Following the usual practice, we adopt this formulation. Briefly, the clusters exhibit redox couple 4;



$$\delta (\Delta E_Q) = 0.55 (3.03) \text{ mm/s (unique subsite)}$$

$$\delta (\Delta E_Q) = 0.51-0.52 (0.68-1.33) \text{ mm/s (other subsites)}$$

the  $\text{P}^{\text{OX}}$  form is reduced at the indicated potential  $E_0'$ .<sup>63</sup> The clusters occur as two slightly inequivalent pairs whose  $\text{P}^{\text{N}}$  forms have the Mössbauer parameters<sup>64</sup> given. Isomer shifts for all subsites are nearly the same, but one subsite is unique because of the large quadrupole splitting, which is closely comparable to that of tetrahedral  $\text{Fe}^{\text{II}}\text{S}_4$  units.

Given the diamagnetic ground state of  $\text{P}^{\text{N}}$ , the two possible redox couples are  $[\text{Fe}_4\text{S}_4]^{+/0}$  and  $[\text{Fe}_4\text{S}_4]^{3+/2+}$  (Figure 10). The redox potential is too low for a normal  $3+/2+$  reaction, and much too high for the  $+/0$  couple based on analogue data.<sup>12</sup> The first

couple could be displaced to lower values by binding of two negative ligands at one or more subsites as in 10-14, and isomer shifts could be raised to the observed values by increased coordination numbers at the subsites. With the  $+/0$  couple, isomer shifts are entirely consistent with a  $[\text{Fe}_4\text{S}_4]^0$  core of a  $\text{Fe}_4\text{S}_4(\text{S}\cdot\text{Cys})_4$  cluster, as is the observation of a transient  $g = 1.94$ -type EPR spectrum corresponding to an unstable  $S = 1/2$   $[\text{Fe}_4\text{S}_4]^+$  species produced during oxidation. Unless the redox step is proton-linked (by, e.g., protonation of the all-ferrous core) or is subject to some special protein environmental effect, it is not clear what displaces the potential upward to the observed value. With either couple, it is also difficult to understand how one subsite of the  $\text{P}^{\text{N}}$  form can be differentiated from the other three by a much larger quadrupole splitting. Indeed, we have yet to produce any  $\text{Fe}_4\text{S}_4$  cluster with a quadrupole splitting as large as 3 mm/s.

In order to accommodate simultaneously the redox potential, ground spin states, and Mössbauer parameters of P-clusters, departure from the ligation mode of a classical  $\text{Fe}_4\text{S}_4(\text{S}\cdot\text{Cys})_4$  cluster appears to be required. The results presented here provide the first comprehensive study of the effects of non-standard terminal ligation in  $[\text{Fe}_4\text{S}_4]^{2+}$  clusters. To provide a more detailed account of these effects, this work is being expanded to oxidized clusters  $[\text{Fe}_4\text{S}_4]^{3+}$  whose potential accessibility in the set 10-14 and with other clusters in dichloromethane solution has already been noted.

- (62) Orme-Johnson, W. H. *Annu. Rev. Biophys. Biophys.* **1985**, *14*, 419.  
 (63) Watt, G. D.; Wang, Z.-C. *Biochemistry* **1986**, *25*, 5196.  
 (64) McLean, P. A.; Papaefthymiou, V.; Orme-Johnson, W. H.; Münck, E. *J. Biol. Chem.* **1987**, *262*, 12900.  
 (65) Smith, B. E.; Lowe, D. J.; Chen, G.-X.; O'Donnell, M. J.; Hawkes, T. R. *Biochem. J.* **1983**, *209*, 207.

**Acknowledgment.** This research was supported by NIH Grant GM 28856, and by the National Science Foundation at M.I.T. G.C.P. acknowledges support by the Office of Naval Research program on Cluster Science and Dynamics under Contract No. N00014-89-J-1779.

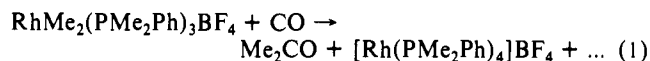
## $\eta^3\text{-MeC}(\text{CH}_2\text{PPh}_2)_3/\text{Rhodium Complexes Utilize Phosphine Arm Dissociation Mechanisms at } 25^\circ\text{C}$

Eric G. Thaler, Kirsten Foltg, and Kenneth G. Caulton\*

Contribution from the Department of Chemistry and Molecular Structure Center, Indiana University, Bloomington, Indiana 47405. Received October 11, 1989

**Abstract:** Reaction of  $\text{RhMe}_3(\text{triphos})$  (triphos =  $\text{MeC}(\text{CH}_2\text{PPh}_2)_3$ ) with CO generates acetone and  $\text{RhMe}(\text{CO})(\text{triphos})$ , which reacts with further CO to give  $\text{Rh}[\text{C}(\text{O})\text{Me}](\text{CO})(\text{triphos})$ . The structure of  $\text{RhMe}(\text{CO})(\text{triphos})$  shows one strained P-Rh-P bond angle between equatorial ligands ( $90.80(5)^\circ$ ) in a trigonal bipyramid, together with intramolecular steric effects that cause a small equatorial CO-Rh-axial(CH<sub>3</sub>) C/C angle of  $79.09(25)^\circ$ . The acetyl and methyl complexes react with  $\text{H}_2$  at  $25^\circ\text{C}$  to produce acetaldehyde and methane, respectively, together with  $\text{RhH}(\text{CO})(\text{triphos})$ . Reaction of CO with  $\text{RhH}_3(\text{triphos})$  is even faster than with  $\text{RhMe}_3(\text{triphos})$  to give  $\text{H}_2$  and  $\text{RhH}(\text{CO})(\text{triphos})$ , together with a CO hydrogenation product. These results show that these clean stoichiometric conversions, as well as a variety of isotopic exchange reactions of the Rh(I) and Rh(III) compounds with  $\text{D}_2$  and  $^{13}\text{CO}$ , occur by preequilibrium dissociation of one arm of the triphos ligand at  $25^\circ\text{C}$ . One such species,  $\text{Rh}[\text{C}(\text{O})\text{Me}](\text{CO})_2(\eta^2\text{-triphos})$ , is directly detectable and reveals the mechanism of exchange of  $\text{Rh}[\text{C}(\text{O})\text{Me}](^{13}\text{CO})(\text{triphos})$  with  $^{12}\text{CO}$ . The coordination of CO to  $\text{Rh}(\text{H})_3(\eta^2\text{-triphos})$  is proposed to generate a dihydrogen complex, thus accounting for the CO-induced elimination of  $\text{H}_2$ . As suggested by these individual reactions,  $\text{RhH}(\text{CO})(\text{triphos})$  is a catalyst for olefin hydroformylation. The high n:iso selectivity mimics that of  $\text{RhH}(\text{CO})(\text{PPh}_3)_3$  in the presence of a large amount of added  $\text{PPh}_3$ , a beneficial consequence of the chelate effect.

We have been examining the polyhydride and polymethyl chemistry of iridium(III) with monodentate phosphine ligands.<sup>1-3</sup> When we attempted to compare these results with the analogous rhodium compounds, the outcome was obscured by phosphine redistribution (eq 1).<sup>4</sup> We reasoned that this problem might be



avoided if we employed the tridentate phosphine  $\text{MeC}(\text{CH}_2\text{PPh}_2)_3$ , "triphos". In addition to "tight" binding (i.e., retention) of phosphine due to the chelate effect, the imposed *facial* stereochemistry of this ligand was anticipated to have major influence

(1) Lundquist, E. G.; Thaler, E. G.; Caulton, K. G. *Polyhedron* **1989**, *8*, 2689.

(2) Rhodes, L. F.; Caulton, K. G. *J. Am. Chem. Soc.* **1985**, *107*, 259.

(3) Alvarez, D.; Caulton, K. G. *Polyhedron* **1988**, *7*, 1285.

(4) Lundquist, E. G.; Streib, W. E.; Caulton, K. G. *Inorg. Chim. Acta* **1989**, *159*, 23.